Université de Montréal

The yeast Rts1, a subunit of PP2A phosphatase, is involved in stress response

Par

Abdelmoez Eshrif

Programme de sciences biomédicales

Faculté de médecine

Mémoire présenté à la Faculté de médecine
en vue de l'obtention du grade de maîtrise en sciences biomédicales
option médecine expérimentale

Décembre 2017

ABSTRACT

The reactive oxygen species (ROS), generated endogenously and exogenously, following treatment with oxidizing agents is well-known to induce double strand deoxyribonucleic acid (DNA) breaks (DDSB). *Saccharomyces cerevisiae* has been used widely as a tool to study the mechanisms that confer sensitivity or resistance to oxidative DDSB repair. Thesis herein describes two separate studies designed to better understand the DDSB repair mechanisms.

The aim of the first study was to assess the role of *rts1*, and its associated genes, in the regulation of oxidative DNA-damage repair mechanisms. The study involved treatment of wild-type (WT) and mutant BY4741 yeast strains with Zeocin, hydrogen peroxide and hygromycin. The nuclear proteins from WT and *rts1*Δ strains were fractionated using fast protein liquid chromatography (FPLC), and the fractions were run on polyacrylamide gel followed by analyses of bands generated or lost using mass spectrometry. Our findings here show an *Apn1*-dependent functional role of *rts1* in DDSB-repair mechanisms. Furthermore, analysis of the FPLC fractions using mass spectrometry revealed up-regulation of *eno1* and down-regulation of *cdc19* following deletion of *rts1*. However, confirmatory experiments only showed significant association of *rts1* with that *cdc19*. Hence, further studies are required to better understand the association of *rts1* with that of *cdc19* and *eno1*, and how their interaction affects the DNA-repair processes and/or cell cycle.

In the second study, we investigated the role of histone H2A in the nuclear localization of Apn1. Furthermore, the study also characterized the role of H2A-E130A residue in methyl methanesulfonate (MMS)-induced DNA-repair response. Out findings herein demonstrated a role for Glu130 residue of Histone H2A in the nuclear localization of Apn1. Importantly, our data also

show the role of the Glu130 in determining the sensitivity as well as the growth rate of the H2A strain to MMS. Future investigation of the *APN1*-related genes will facilitate better understanding of the role of Apn1 and its associated genes in regulating the repair mechanisms following double strand DNA breaks induced by alkylating agents.

Key words: Protein phosphatase 2A, Zeocin, Rts1, Cdc19, Histone H2A, Apn1, Chromosomal DNA, NLS, AP sites

RÉSUMÉ

Les espèces réactives de l'oxygène (ROS), générées de manière endogène, et de maniére exogène suite à un traitement avec des agents oxydants, sont bien connues pour induire des cassures doubles brin (DDSB) de l'acide désoxyribonucléique (ADN). *Saccharomyces cerevisiae* a été largement utilisée comme outil pour étudier les mécanismes qui confèrent une sensibilité ou une résistance à la réparation oxydative du DDSB. La thèse décrit deux études distinctes conçues pour mieux comprendre les mécanismes de réparation du DDSB.

Le but de la première étude était d'évaluer le rôle de rts1 et de ses gènes associés dans la régulation des mécanismes de réparation des dommages oxydatifs de l'ADN. L'étude a impliqué le traitement de souches de levure BY4741 de type sauvage (WT) et des souches mutantes avec de la zéocine, le peroxyde d'hydrogène et de l'hygromycine. Les protéines nucléaires des souches WT et rts1Δ ont été fractionnées en utilisant la chromatographie liquide de protéine rapide (FPLC). Les fractions ont été passées sur un gel de polyacrylamide suivi par des analyses de bandes générées ou perdues en utilisant la spectrométrie de masse. Nos résultats ici montrent un rôle fonctionnel d'Apn1 dans les mécanismes de réparation DDSB, dépendamment de rts1. En outre, l'analyse des fractions de FPLC a révélé une augmentation de eno1 contre une diminution de cdc19 après la suppression de rtsl. Cependant, les expériences de confirmation ont montré qu`une association significative de rts1 avec CDC19. Par conséquent, d'autres études sont nécessaires pour mieux comprendre l'association de rts1 avec celle de cdc19 et eno1, et comment leur interaction affecte les processus de réparation de l'ADN et / ou le cycle cellulaire.

Dans la deuxième étude, nous nous sommes intéresses au rôle de l'extrémité N-terminale de l'histone dans la localisation nucléaire de Apn1. L'étude a également caractérisé le rôle du résidu H2A-E130A dans la réponse à la réparation des dommages de l'ADN induits par le méthanesulfonate de méthyle (MMS). Les résultats ont démontré un rôle du résidu Glu130 de l'histone H2A dans la localisation nucléaire de Apn1. Nos données montrent également le rôle de la Glu130 dans la détermination de la sensibilité ainsi que le taux de croissance de la souche H2A au MMS. Une étude future des gènes associés à Apn1 facilitera une meilleure compréhension du rôle de cette protéine et de ses gènes associés dans la régulation des mécanismes de réparation des cassures double brin de l'ADN induites par les agents alkylants.

Mots clés: Protéine phosphatase 2A, Zeocin, Rts1, Cdc19, Histone H2A, Apn1, ADN chromosomique, NLS, Sites AP.

Table of contents

ABSTRACT…… ii

RÉSUMÉ……... iv

Table of contents…….... vi

List of figures……..... ix

List of tables…….....x

Abbreviations list……... xi

Acknowledgement……. xiv

CHAPTER ONE: ……. ….....1

1. Literature Review…….....1

1.1 Cancer: Epidemiology and Etiology…….....1

1.2 Cancer Treatment and Resistance…….....2

1.3 Saccharomyces cerevisiae in Cancer Therapeutics…….....4

1.3.1 S. cerevisiae and Oxidative DNA damage …….....5

1.3.1.1. Base Excision Repair: The primal role of APN1…….....6

1.4 Role of RTS1 in Cell Cycle……...7

1.5 Histone H2A and APN1…….7

1.6 Hypothesis…….9

1.7 Objectives.....9

CHAPTER TWO. ……..……...10

2. Materials and Methods……...10

2.1. Yeast strains and growth media……...10

2.2 Rapid Approach to DNA Adduct Recovery (RADAR) Assay…….…….....10

2.3 Nuclear protein extraction for fast protein liquid chromatography……...12

2.4 Western Blot…….....12

2.5. Silver staining…….…….....13

2.6. Mass spectrometry……...14

2.7 Survival curve……...14

2.8 Spot test……14

2.9 Delta Vision microscopy……..15

2.10 Growth Curve Assay……..15

CHAPTER THREE. …….....…….…….....16

3. First study results…….....…….…….....16

3.1 Role of RTS1 and its associated genes in regulating DNA-repair response…….16

3.1.1 Zeocin0-induced DNA-damage reduces the nuclear recruitment of RTS1 ……...…16

3.1.2 Zeocin-induced DNA-damage reduces the survival of RTS1……17

3.1.3 H_2O_2-induced oxidative stress reduces the nuclear recruitment of RTS1…….....17

3.1.4 Protein Purification and Evaluation of RTS1-related proteins …….....18

3.1.5 Generation and validation of CDC19 and ENO1-related strains……19

3.1.6 Deletion of RTS1 reduces the expression of ENO1…….....23

3.1.7 Possible Role of RTS1 Gene in modulation the expression of CDC19……...…..24

CHAPTER FOUR. ……....27

4. Second study results……..…….27

4.1 Role of Histone H2A-E130A residue in recruiting Apn1……....27

4.1.1. H2A-E130A mutant prevents localization of Apn1 to the nucleus……....27

4.1.2. H2A- E130A mutant is sensitive to MMS…….....27

4.1.3. Knockdown of APN1 increases the sensitivity to MMS and decreases the life span of H2A-E130A strain…….……..……....29

CHAPTER FIVE…….……. …….....32

4. DISCUSSIONS and CONCLUSIONS……...…....32

4.1 Role of RTS1 and its associated genes in regulating DNA-repair response…….....32

4.2 Role of Histone H2A-E130A residue in nuclear localization of Apn1…….…….37

References……..40

List of figures

Figure 1. Effect of Zeocin on the recruitment of Rts1 to the DNA.

Figure 2. Survival Curve of Zeocin (25μg/ml) treated WT, rts1Δ, rad51Δ, rts1Δrad51Δ strains.

Figure 3. Effect of H_2O_2 treatment on the recruitment of Rts1 to DNA.

Figure 4. Silver stained polyacrylamide gel of fractions #22 and 23 extracted from BY4741 WT and –rts1Δ strains.

Figure 5. Analysis of PCR end products to confirm the deletion of RTS1 gene.

Figure 6. Validation of the BY4741 (A) CDC19-TAP and CDC19-TAP-rts1Δ, and (B) CDC19-MYC strains using anti-PAP and anti-MYC antibodies, respectively.

Figure 7. rts1 Gene Deletion Reduces ENO1 Expression.

Figure.8. Expression levels of CDC19 in untreated and Hygromycin (25 μg/ml)-treated BY4741-CDC19-Myc and BY4741-CDC19-Myc-rts1Δ strains.

Figure 9. Quantification of the expression levels of CDC19 in the untreated and Hygromycin (25 μg/ml)-treated BY4741-CDC19-MYC and BY4741-CDC19-MYC-rts1Δ strains.

Figure 10. Differences in the nuclear localization of APN1 in H2A and H2A-E130A cell strains.

Figure 11. Expressional levels of APN1 in the nucleus of H2A and H2A-E130A strains.

Figure 12. Sensitivity of H2A WT and H2A-E130A strains to MMS.

Figure 13. H2A-E130A mutant strain has increased sensitivity to MMS following deletion of apn1

Figure 14. Deletion of apn1 affects the survival rate of the H2A-E130A-apn1Δ strain.

List of tables

Table 1. Primers used to create mutant strains.

Table 2. The list of highly expressed proteins of Fraction #23, determined using mass spectrometry, from the band lost (~60 KDa) in the rts1Δ strain.

Table 3. The list of highly expressed proteins of Fraction #23, determined using mass spectrometry, from the new band generated (~37 KDa) in the rts1Δ strain.

Abbreviations list

3′-dRP	3′-deoxyribosephosphate

AP:	Apurinic/apryrimidic site
Apn1	AP-endonuclease 1
Apn2	AP-endonuclease 2
BER	Base Excision Repair
BLM:	Bleomycin
BRCA1	Breast cancer gene 1
BRCA2	Breast cancer gene 2
CDC19	Pyruvate kinas
Cdc55	PP2A subunit
Cdc9	DNA ligase I
Cln2	Neuronal ceroid lipofuscinosis type 2
D10b	E coli Bacteria
DDSB	DNA double strand break
DNA	Deoxyribonucleic acid
DTT	Dithiothreitol
EDTA	Ethylene Diamine Tetra-Acetic
Eno1:	Endonucease1
Fe^{2+}	Ferrous ion
FPLC	Fast protein liquid chromatography
GFP	Green Fluorescent Protein
Glu130	Glutamates amino acid at 130 residue

GTC	Guanidine Thiocyanate
H2AX	A member X of H2A histones family,
H2O2	Hydrogen peroxide
HEPES	4-(2-hydroxyethyl)-1-piperazineethanesulfonic acid
HOG	High Osmolarity Glycerol Response MAP Kinas
HR	Homologous recombination
HRR	Homologous Recombination Repair
KPB	Potassium phosphate buffer
MB	RADAR Assay lysis solution
MIB	3--Morpholinoisoborneol
MLH1	Human mutL homolog 1
MMS:	Methyl methanesulfonate
MS	Mass Spectrometry
MSH2	MutS protein homolog 2
NER	Nucleotide Excision Repair
NLS	Nuclear localization signal
PAP	Peroxidase Anti Peroxidase
PCR	Polymerase chain reaction
PMSF	Phenylmethylsulfonyl fluoride
Pol-II	RNA Polymerase II

PP2A	Protein phosphatase 2A
Rad27	(Fen-1) nuclease
RAD51	DNA recombination / repair protein
RNA	Polymerase II holoenzyme (RNAPII)
RNA:	Ribonucleic acid
ROS	Reactive Oxygen Species
RT	Room Temperature
Rts1	B-type regulatory subunit of protein phosphatase 2A
SDS	Sodium Dodecyl Sulphate
TAP	Tandem affinity purification
TBS-T:	Tris-buffered saline with Tween
TCA	Trichloroacetic acid
URA3	Encodes Orotidine-5'-phosphate (OMP) decarboxylase
WT	Wilde Type
Yap1p	Basic leucine zipper (bZIP) transcription factor
YPD	Yeast culture media (Yeast extract Peptone – Dextrose)

Acknowledgements

My thesis will never exist to the reality without the kind support of many individuals, I would like to extend my sincere thanks to all of them.

Foremost, I would like to express my gratitude towards my research director Prof. Dindial Ramotar for his support, pleasant times in the lab, helpful discussions and comments.

I would like to send special greetings and special invitations to my father's spirit in his grave for his previous support and encouragement before his death. I also wish to express my sincere thanks to My entire family, my mother for their love, support and encouragement. I want to thank my siblings as well as my future wife Mariam.

I place on record, my sincere gratitude to faculty of medical technology, university of Zawia and the Libyan ministry of education for their constant encouragement and for their finical support.

I would like to thank Prof. Yahye Merhi, the head of the department of Biomedical science, university of Montreal for his constant availability and your advice and encouragement during. I also want to thank the committee members for evaluating my thesis and for their relevant comments and suggestions that improve my research

Finally, I would like to thank everyone who I have crossed paths with during my thesis and that helped me get through my graduate studies. I would like to than their helps with my experiments in project.

CHAPTER ONE: Literature Review

1. Literature Review

1.1 Cancer: Epidemiology and Etiology

Cancer is a major cause of morbidity and mortality in both developed and developing countries (Fidler et al. 2017). To date, over two hundred types of cancer have been identified. Among these, the most common types are carcinomas of the breast, lung, prostate and bowel (Ferlay et al. 2015). It has been estimated that cancer causes more deaths than cardiovascular diseases or stroke (Fidler et al. 2017). In 2012, the GLOBOCAN project estimating worldwide cancer incidence and mortality reported 14.1 million new cancer cases and 8.2 million cancer-related deaths (Ferlay et al. 2015). Gender as well as demographic differences in the incidence and prevalence of various cancers has also been documented (Ramotar et al. 1993, Fidler et al. 2017).

Cancer, a term used to describe a group of co-morbid diseases, is characterized by abnormal and/or uncontrolled cell growth (Lee et al. 2016). Somatic cells divide regularly throughout the life span of an individual governed by a tightly-regulated sequence of events, collectively termed cell cycle process (Hanahan and Weinberg 2011). This homeostatic pathway ensures proper maintenance of cell growth and function (Hanahan and Weinberg 2011). Under normal physiology, cells determined with non-repairable defects or mutations during cell-cycle checkpoints are programmed for apoptosis (Hanahan and Weinberg 2011). However, certain deoxyribonucleic acid (DNA) mutations can make cells resistant to apoptosis, resulting in faster replicating abnormal cancerous or neoplastic cells (Hanahan and Weinberg 2011). The hallmark characteristic features of cancer cells include, sustained proliferation, evasion of growth suppressors, resistance to

apoptosis, replicative immortality, sustained angiogenesis, primary and secondary metastasis, evasion of immune system, but to name a few (Hanahan and Weinberg 2011).

The etiology of cancer encompasses several genetic, epigenetic and environmental factors (Migliore and Coppede 2002). Genome wide association studies have identified several cancer susceptibility genes, including *BRCA1, BRCA2, MLH1 and MSH2*, with high penetrance for breast, ovarian and colorectal cancers (Sud, Kinnersley, and Houlston 2017). In particular, genetic polymorphism or mutations of various genes involved in DNA repair, tumor-suppressor, and proto-oncogenes genes are well known to facilitate neoplastic changes (Aunoble et al. 2000). Environmental factors such as ionizing radiation, alcohol, viruses, chemicals, tobacco products and pollutants are some of the potential carcinogenic agents (Parsa 2012). Specifically, tobacco smoke and alcohol products contributes to as many as half of all cancer deaths in the United States (Lee and Hashibe 2014).

1.4 Cancer Treatment and Resistance

The therapeutic armamentarium for metastatic cancers encompasses a wide range of pharmacological as well as non-pharmacological approaches. These include radiation therapy, chemotherapy, surgery, hormone therapy and immunomodulatory therapy (Nussbaumer et al. 2011). However, much of the existing anti-cancer therapies are restricted by poor efficacy, cancer-cell selectivity and/or dose-limiting side-effects (Nussbaumer et al. 2011). The persistent increase in the annual number of newly diagnosed cancer patients as well as cancer-related deaths (Torre et al. 2015) has urged the need for well-tolerated novel anti-cancer medications.

Over the past three decades, vast research advancements have been made to facilitate our understanding of the molecular mechanisms underpinning the development and/or maintenance of various human cancers (Narang and Desai 2009). Anti-cancer drug discovery programs around the globe have identified a number of molecular targets, related to cancer prognosis, growth, and/ or metastasis (Narang and Desai 2009). Targeting these cancer-specific molecular targets will also avoid unwanted physiological effects on normal somatic cells. However, the low success rate, together with significant cost and time involvement, of these candidate molecules have necessitated the use of high throughput preclinical screening methods and biological assays with greater specificity and predictability (Nussbaumer et al. 2011).

Further to the afore-mentioned challenges, a major impediment to successful development of anti-cancer therapeutics is the development of therapeutic resistance, which in some cases predates clinical intervention (Zahreddine and Borden 2013). In particular, resistance to chemotherapeutic agents, a gold standard therapeutic regimen for various cancers, is commonly observed in the clinical setting (Gatenby 2009). Cancer resistance is primarily classified as two types, viz. intrinsic and acquired resistance, based on the response of the tumor to initial anti-cancer therapy (Lippert, Ruoff, and Volm 2011). Intrinsic resistance is the inherent ability of the cancer cells to be resistant to traditional anti-cancer therapeutics, and has been recognized in ~50% of all cancer patients (Zahreddine and Borden 2013). The presence of cancer stem cells, which constitutively express drug transporters, DNA repair genes and are resistant to apoptosis, have been attributed towards intrinsic cancer resistance (Lou and Dean 2007). In contrast, acquired resistance is the characteristic feature of cancer cells to display little or no response, following prolonged drug treatment, through somatic genetic changes (Meads, Gatenby, and Dalton 2009). Both intrinsic

and acquired resistance can be caused due to alterations to drug metabolism or modifications of drug targets (Ullah 2008, Zahreddine and Borden 2013).

1.3 *Saccharomyces cerevisiae* in Cancer Therapeutics

The completion of genome sequences as well as myriad genetic tools, that facilitate somatic cell genetics, have resulted in the advent of non-mammalian models (e.g., Drosophila, yeast, zebrafish etc.) for cancer drug discovery and development programs (Sherman 2002, Paddison and Hannon 2002). Among these, the ability of *Saccharomyces cerevisiae* to propagate in haploid as well as diploid state, coupled with the high degree of conservation of basic cell cycle machinery, render the *S. cerevisiae* particularly invaluable for cancer therapeutic studies (Bjornsti 2002). On a particular note, ~17% of *S. cerevisiae* genes are members of orthologous gene families associated with human diseases, making it a valuable model organism (Dolinski and Botstein 2007).

The facile classic genetic manipulation of this budding yeast has been used widely in understanding the genes involved in metabolic pathways and/or cell cycle checkpoint functions (Bjornsti 2002). Importantly, the characteristic insensitivity of these yeast cells to many chemotherapeutic agents (Bjornsti 2002) can be exploited to define the role of specific genetic defects that potentiate therapy-induced cytotoxicity. This, combined with the high degree of conservation of DNA repair pathways (Simon et al. 2000), makes budding yeast an excellent model to study the genes involved in conferring sensitivity and/or resistance to therapeutic agents that induces DNA damage.

1.3.1 *S. cerevisiae* and Oxidative DNA damage

Like any other living cells, *S. cerevisiae* are exposed to stress due to reactive oxygen species (ROS), nutrient imbalance, temperature fluctuations, pH variation and exposure to toxic chemicals (Folch-Mallol et al. 2004). Specific pathways in response to oxidative, osmotic and heat stress include a) Yap1p and Yap2p transcription, (b) HOG kinase pathway and (c) heat shock factor, respectively (Folch-Mallol et al. 2004). Subsequent to the sensation of stress, appropriate response is conveyed through repression of catabolites, amino acid regulation and nitrogen regulation (Attfield 1997). The oxidative stress caused by the ROS generated endogenously and exogenously results in DNA damage, thereby affecting cell viability. In order to better understand the molecular mechanisms underlying oxidative DNA damage repair, various oxidizing agents such as heavy metals (e.g., selenium, chromium etc.), methyl methanesulfonate (MMS) and Bleomycin have been used to induce double stranded DNA breaks (DDSB) (Pinson, Sagot, and Daignan-Fornier 2000, Litwin, Dziadkowiec, and Wysocki 2013, Kitanovic et al. 2009).

Bleomycin (BLM) and its related family of compounds (e.g. Zeocin) are well known for their anti-cancer and antibiotic properties (Chen et al. 2008). The anti-tumor effect of BLM is exerted through oxidative lesions in chromosomal DNA, formed via a complex that is produced when BLM binds to iron (Fe^{2+}) and oxygen *in vivo* (Bugaut et al. 2013). The activated Fe-BLM complex takes a hydrogen atom from the be C4' carbon of the 2-deoxyribose moiety, resulting in two types of lesions: (i) oxidized apurinic/apyrimidinic (AP) sites and (ii) DNA single-strand breaks that terminate with 3-phosphoglycolate (Chen et al. 2008). Although DNA lesions produced by BLM-oxidative damage is repaired by the base excision repair (BER) and nucleotide excision repair

(NER) pathways, the nature of damage and the phase of cell cycle determines activation of appropriate pathways (Boiteux and Jinks-Robertson 2013).

1.3.1.1. Base Excision Repair: The primal role of APN1

The BER is considered as the primary DNA repair pathway against lesions arising from alkylation, oxidation, depyrimidination, and deamination (Hoeijmakers 2001). The resultant DNA lesions are repaired by the actions of DNA N-glycosylases and apyrimidinic/apurinic (AP) endonucleases. Briefly, the BER is initiated by the cleavage of the N-glycosylic bond between the damaged base and the sugar moiety by the *N*-glycosylase enzyme, resulting in formation of an AP site (Chalissery et al. 2017). Subsequently, a single strand break is formed with the 3′-deoxyribosephosphate (3′-dRP) ends, which are removed by the AP endonucleases, viz. Apn1 and Apn2 (Popoff et al. 1990). Previous studies have shown that the deletion of the *Apn1* increases the rate of spontaneous mutations and renders the cell sensitive to DNA damage induced by H_2O_2 and MMS (Ramotar et al. 1991, Johnson et al. 1998). Furthermore, Apn1 has been demonstrated to be functionally independent of the various DNA N-glycosylases lyases (e.g., Ntg1/2, Ogg1) involved in the BER pathway (You et al. 1999). Importantly, *apn1* mutants devoid of nuclear localization signal resulted in the strains inability to complement the sensitivity of apn1 deficient strain to H_2O_2 and MMS (Ramotar et al. 1991, Johnson et al. 1998). Thus, Apn1 is the major multifunctional nuclease involved in the repair of oxidatively damaged mitochondrial as well as nuclear DNA (Acevedo-Torres et al. 2009). Further actions of DNA polymerase ε and δ, endonuclease Rad27 and DNA ligase Cdc9 completes the BER of the damaged DNA (Chalissery et al. 2017).

1.4 Role of RTS1 in Cell Cycle

The canonical protein phosphatase 2A (PP2A) is a heterotrimeric complex composed of a catalytic subunit (C), a scaffolding subunit (A), and a regulatory subunit (B) (Zhong et al. 2014). In mammals, PP2A is a major intracellular protein that regulates cell growth and metabolism, and contains multiple isoforms of the B-regulatory subunit (Janssens and Goris 2001). In stark contrast, there are only two B-regulatory subunits, referred to as Rts1 and Cdc55, in budding yeast.

The diversity of B subunits in the PP2A heterotrimer allows to localize phosphatase to distinct regions of the cell and to dephosphorylate specific substrates. As such, this enables PP2A to regulate diverse cell processes including DNA replication (Li and Virshup 2002). Previous works by others have shown that yeast strains that lack *RTS1* are sensitive to temperature, ethanol and glycerol (Jiang 2006, Petty et al. 2016), and failed to undergo nutrient modulation of cell size (Artiles et al. 2009). Disruption of the *RTS1* gene has been shown to delay transcription of G1 cyclin Cln2, thereby prolonging mitosis and affecting cell cycle progression (Zapata et al. 2014). A role for Rts1 has also been shown in abrogation of spindle position checkpoint, but not in other mitotic checkpoints (Chan and Amon 2009). Together, these findings suggest a role for Rts1 in both G1 and mitotic cell size checkpoints. However, the role of Rts1 in the modulation of DNA-oxidative damage is unknown. Hence, we propose to investigate the role of Rts1 in Zeocin mediated DDSB response, alongside with Apn1 whose role is well-established in DDSB repair.

1.5 Histone H2A and APN1

As already noted in *Section 1.3.1.1*, Apn1 plays a vital role in the initiation and maintenance of the BER pathway in response to DDSB. However, for effective DDSB repair, the BER pathway

must also have access and act upon the chromatin containing the damaged DNA (Soria, Polo, and Almouzni 2012).

Histones are monomeric building blocks of chromatin involved in eukaryotic DNA packaging and organizing into nucleosomes (Richmond 1999). The types of core histones include H1, H2A, H2B, H3, and H4 (Bonisch and Hake 2012). The Histone H1 takes part in chromatin's higher order structure, while the rest of the canonical histones are incorporated into chromatin during DNA replication through the action of histone chaperones (Williamson et al. 2012). Among canonical histones, the H2A family, comprising H2AX and H2AZ variants, exhibits highest sequence divergence and are associated with DDSB-repair (Williamson et al. 2012).

The canonical histone proteins, namely H2A, H2B, H3 and H4, share a common structural domain that consists of 3 α-helices and two β-strands (α1–β1–α2–β2–α3–αC) (Venkatesh and Workman 2015). The α-helices are separated by two loops, called the histone fold, which facilitates heterodimerization of H2A with H2B and H3 with H4 (Venkatesh and Workman 2015). Each of the canonical histones contains an unstructured amino-terminal tail that facilitates intra- and inter-nucleosomal interactions (Zheng and Hayes 2003). In response to DNA damage, the these N-tails of histones extend out of the nucleosome core are post-translationally modified (Meas, Smerdon, and Wyrick 2015b). Additionally, it has been shown that the N-tail pairs are redundant for cell viability (Kim et al. 2012). Furthermore, N-tail deletions of various histones have been shown to be sensitive to alkylating agents (Meas, Smerdon, and Wyrick 2015a). Given the role of H2A in DDSB-repair (Venkatesh and Workman 2015), and the role of N-terminal of histone in facilitating inter-/intra-nucleosomal interactions (Zheng and Hayes 2003), it is possible that the N-terminal of

histone may be involved in the recruitment of Apn1 via its interaction with the C-terminal of APN1.

1.6 Hypothesis

1. Rts1 is a component of PP2A. Mutants are sensitive to temperature, osmotic stress, and bleomycin, yet resistant to methylation. Nuclear extraction and MS analyses identified two proteins by comparing Rts1 WT and mutants (Cdc19 and Eno1)
2. The Glu130 in the Histone H2A is required for the nuclear localization of Apn1. The same residue is also responsible in determining the sensitivity of the H2A yeast strain to methyl methanesulfonate (MMS).

1.7 Objectives

The study aims to investigate the role of Rts1, and its associated genes, in the regulation of Zeocin- and hygromycin-related DNA-damage repair mechanisms.

1. To assess if the of histone H2A his involved in the nuclear localization of Apn1 via its interaction with the C-terminal of Apn1. Furthermore, the study also aims to characterize the role of H2A-E130A residue in MMS-induced DNA-repair response.

CHAPTER 2. MATERIALS AND METHODS

2. Materials and Methods

2.1. Yeast strains and growth media

The experiment included a number of yeast wild-type (WT) and mutant strains. The yeast strains, such as BY4741-RTS1-TAP, BY4741-*rad51*Δ, BY4741-*rts1*Δ*rad51*Δ, H2A-WT-APN1-GFP, H2A-E130A and H2A-E130A-APN1-GFP, used in the experiments herein were created previously in our laboratory. Yeast strains, including BY4741-*rts1*Δ, BY4741-CDC19-MYC, BY4741-ENO1-TAP-*rts1*Δ, BY4741-CDC19-MYC-*rts1*Δ, H2A-E130A-APN1-TAP and H2A-WT-APN1-TAP were created using polymerase chain reaction (PCR) technique (Table 1). The yeast strains, viz. BY4741-CDC19-TAP, BY4741-ENO1-TAP, were procured from a different laboratory. As previously described, yeast cells were grown either in yeast extract-peptone-dextrose (YPD) growth media containing 1% Yeast Extract (MULTICELL), 2% peptone (BIO BASIC INC), and 2% dextrose (BIO BASIC INC), or selective media containing 0.75% Yeast Nitrogen Base (3.25g in 500ml) (DIFCO) and 2% dextrose (BIO BASIC INC), supplemented with the amino acids necessary for cells growth depending on the genotype. Solid media was obtained by the addition of 2% Agar and 1.5% LB Agar.

2.2 Rapid Approach to DNA Adduct Recovery (RADAR) Assay

Yeast strains were grown overnight in 1ml YPD liquid media at 30°C. The following day, the cells were sub-cultured in 3ml YPD (cell to media - 1:3 ratio) at 30°C for 3 hours, and treated with Zeocin, methyl methanesulfonate (MMS) or hydrogen peroxide (H_2O_2). The treated or untreated (control) cells were then extracted using M buffer (RADAR lysis solution containing 4M Guanidine Thiocyanate (GTC), 10mM Tris-HCl PH 6.5, 20mM EDTA, 4% Triton 100X and 1%

Sodium lauroyl Sarcosinate (Sarkosyl)). The extracted sample was then centrifuged to collect the cell pellet, where GTC captures the proteins around DNA.

Table. 1 Primers used to create mutant strains.

Name	**Primer Sequence (5' -> 3')**
RTS1-F	CGCTTTGTTTTCCACTTCAATTGGTAGGC
RTS1-R	CGGGGATTCTATCTTTGGTTTCTTCAACAAG
pTW438-CDC19-F	TGCACAATATTTCAAGCTATACCAAGCATACAATAAGCT TATGTCTAGATTAGAAAGATTGACCTCATTAAACGT
pTW438-CDC19-MYC-R	AATGAGCTTTTGCTCGGACGCCATGGTGAGAACGGTAGA GACTTGCAAAGTGTTGGAGTGACCAGCACCGGCCTT
H2A-Apn1-F	CTATGCTTAGGAATAACGTTCG
H2A-Apn1-R	AAGTCAAAAGGGAAGATG

Ethanol was used to precipitate nucleic acids and the protein concentration was quantified using Bradford Assay in the resultant DNA-associated proteins. The samples were then diluted with Tris-buffered saline (TBS; 10 mM Tris (pH 6.8), 150 mM NaCl) to similar protein concentrations (800 ng/µl) and loaded on nitrocellulose membrane using a vacuum slot-blot manifold (Bio-Rad). The membranes were then blocked for 1h in 5% milk-TBST and incubated with appropriate primary antibodies in TBST (1:2500) overnight at 4°C. Following 3 X 5min wash with TBST, the membranes were incubated with appropriate secondary antibodies (1:1000) for 1h at room temperature (RT). Membranes were then scanned using a ImageQuant Las 4000.

2.3 Nuclear protein extraction for fast protein liquid chromatography

Yeast cells were grown overnight in 500ml of YPD liquid media. The following day, 300ml of each sample was centrifuged at 3000xg and the resulting cell pellet was weighed and washed with distilled water. The cells were then re-suspended in Tris buffer (pH 9.4) containing 10mM DTT (0.3g/ml) and incubated at 30 °C for 10min. Subsequently, the samples were centrifuged at 3000xg and washed with Buffer B (1.2 M D-sorbitol, 20 mM KPB pH 7.4; 1 ml of Buffer B per 0.1g of cell pellet). Zymolase (2.5µl/g of cell pellet) was then added and the samples were incubated at 30 °C for 60min with gentile agitation. Following further centrifugation and washes with buffer B (1g /10ml), the cells were re-suspended in MIB reagent (27.3g of Monitol + 50ml of HEPES 100mM in 250ml final volume) followed by addition of 0.5 mM Phenylmethylsulfonyl fluoride (PMSF). The samples were then homogenized using a glass syringe and centrifuged at 3000xg for 5min. The resultant nuclear extracts were run on a Fast protein liquid chromatography (FPLC) and fractions were analyzed by western blot (Nassour et al. 2016).

2.4 Western Blot

Western Blot technique was used for both total extraction as well as nuclear extraction for FPLC filtered fractions. For total extraction, the cells pellet from overnight grown cells in YPD media was extracted by 20% Trichloroacetic acid (TCA) extraction or by standard extraction method. In TCA extraction, the samples were vortexed for 10min and then centrifuged. The cell pellet was mixed with 5µl of loading buffer containing mercaptoethanol and the proteins were denatured by heating for 5min at 100°C. In contrast, for standard extraction, total extract was obtained by vortexing the samples for 10min at 4°C followed by centrifugation for 3min at 3000rpm in an Eppendorf centrifuge. The supernatant was then collected for quantification using Bio-Rad Protein

Assay. Following protein quantification, equal amounts of extracted sample was mixed with loading buffer (50mM Tris-HCl pH 6.8, 2% SDS, 0.1% bromo-phenol blue, 2% (v/v) 2-mercaptoethanol). Following FPLC, the filtered samples were quantified using NanoDrop, mixed with 5µl of loading buffer and the proteins were denatured by heating for 5min at 100°C. The denatured protein samples obtained by both the extraction methods were then loaded onto a 10% Sodium dodecyl sulfate (SDS) polyacrylamide gel. The proteins were then transferred onto a nitrocellulose membrane. The membrane was blocked for 30min with 5% skim milk in TBST (10mM Tris-HCl (pH 7.5)-150mM NaCl-0.1% Tween) then incubated overnight at 4°C with the mouse monoclonal anti-MYC antibody (1:5000 in 5% milk). Following washes (10min each) with TBST, the membrane was incubated for 1h with the Goat anti-mouse antibody (1:2500). Finally, the membranes were incubated for 1min in chemiluminescence reagent and developed using a Fujifilm ImageQuant Las 4000.

2.5. Silver staining

The silver staining was undertaken according to previous published protocols (Chevallet, Luche, and Rabilloud 2006). Briefly, the SDS polyacrylamide gel with protein (from FPLC fractions) was incubated with a fixative solution (40% MetOH, 10% GGA in water) for 20min in a glass tray. The gel was then washed with 30% ethanol and water (20min each). Subsequently, the gel was incubated for 20min with a staining solution (500 mg of Silver nitrate, 50 µl of formaldehyde 250ml of Water) in a bottle wrapped with aluminum. The silver stain was then reduced in 0.01% sodium thiosulfate. The gel was then washed with water and developed (100ml developer solution; 10g of sodium carbonate and 100µl of formaldehyde). Following visibility of a band, the reaction was stopped using 5% acetic acid.

2.6. Mass spectrometry

Protein bands were cut from the silver stained gels and stored in 200µl of distilled water. The samples were then for mass spectrometry analysis to Ross Tomaino Lab Harvard (Boston, USA).

2.7 Survival curve

In survival curve assay, the BY4741-WT, -*rts1*Δ, -*rad51*Δ and -*rts1*Δ*rad51*Δ cells were grown in 1ml YPD media overnight and sub-cultured for 3 hours in 2 ml YPD media. The cells were then washed with distilled water. The cell density was quantified at 600nm wavelength. The cells of same density were treated with YPD for different concentrations of Zeocin (25 – 75 µg/ml) and incubated for different time points (15, 30, 45 min) at 30°C with shaking (150 RPM) for 1h. The cells were then diluted with YPD media ($1:10^{-1}$, $1:10^{-2,}$ $1:10^{-3}$ and $1:10^{-4}$) on 96 well-plate. The survival was then determined, as previously described (Yang et al. 2012), by plating 100µl of serial diluted cells onto selective minimal media plates. The cell colonies were counted after two days of growth at 30 °C.

2.8 Spot test

The H2A-WT, -*Apn1*Δ, -E130A and -E130A-*Apn1*Δ strains were grown overnight in 2 ml of YPD liquid media at 30°C. The following day, cells were sub-cultured in 1:3 ratio in YPD liquid on the shaker at 30 °C. After 3 hours, optical density was measured at 600nm and several dilutions were prepared. From each strain, 5µl of sample was spotted manually on YPD agar plates along with different concentration of MMS, as previously described by (Sisakova et al. 2017). The agar plates were incubated for two days at 30°C before being photographed by the Alphaimager®.

2.9 DeltaVision microscopy

The H2A-WT and -E130A mutant strains were grown overnight in YPD. The subsequent day, cells were washed and fixed with formaldehyde. The concanavalin A was used to adhere the cells on slides and the pictures were taken by an Olympus Delta Vision microscope at 100x. The Since Apn1 C-terminal was tagged with GFP, FITC filter was used while imaging. The cells were also co-stained DAPI to visualize nuclei.

2.10 Growth Curve Assay

The H2A-WT, -E130A, -*apn1*Δ and -E130A-*apn1*Δ strains were grown overnight in YPD and the optical density was determined at 0.2 in 96 microplates. Some strains were treated with a minimal dose of MMS (0.0025 μg/ml) and incubated at 30°C for up to 17 hours in the instrument where readings were automatically every 30min. The data was then analyzed data using Microsoft Excel 2016.

CHAPTER 3. First study results

3.1 Role of *RTS1* and its associated genes in regulating DNA-repair response

3.1.1 Zeocin-induced DNA-damage reduces the nuclear recruitment of RTS1

This experiment investigated the effect of Zeocin (50µg/ml), a double stranded DNA-breaking agent, on the expression levels of APN1 (anti-APN1 antibody) and TAP tagged RTS1 (detected using anti-PAP antibody) in the BY4741-RTS1-TAP and BY4741-WT cells. The expression levels of APN1 in the BY4741 WT cells were not significantly affected by the Zeocin treatment (Figure 1). In contrast, the BY4741-RTS1-TAP cells treated with Zeocin showed significant time-dependent reduction in the expression levels of RTS1, as detected by the anti-PAP antibody (Figure 1). Interestingly, there was a time-dependent decrease in the expression levels of APN1 in the BY4741-RTS1-TAP cells following Zeocin treatment (Figure 1).

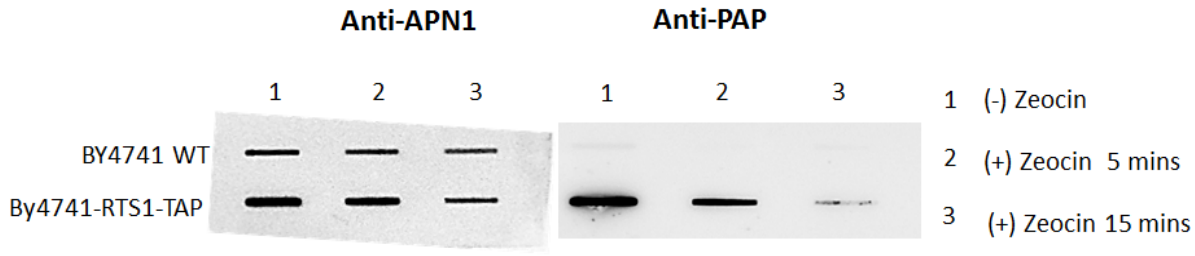

Figure 1. Effect of Zeocin on the recruitment of Rts1 to the DNA. Treatment of the BY4741 WT cells with Zeocin at 50µg/ml did not affect the levels of APN1, suggesting the role of APN1 in DNA double strand break (DDSB) repair. The TAP tagged BY4741-RTS1, but not BY4741 WT, cells showed visible bands for anti-PAP as a secondary antibody, validating the presence of the tag. Treatment of BY4741-RTS1-TAP cells with Zeocin significantly reduced the levels of RTS1 (TAP tagged) in a time-dependent manner. Interestingly, there was a reduction in the levels of Apn1 following treatment of BY4741-RTS1-TAP cells with Zeocin.

3.1.2 Zeocin-induced DNA-damage reduces the survival of RTS1

Next, we assessed the role of Rts1 in cell survival following treatment with Zeocin. Our data herein show that the *rts1*Δ strains were ~25% more sensitive than the WT strain to Zeocin treatment (Figure 2). The *rad51*Δ strain displayed reduced survival following Zeocin treatment c.f. Zeocin treated WT or *rts1*Δ strains (Figure 2). The mutant strains with deletion of both *RAD51* and *RTS1* genes displayed hypersensitivity to Zeocin (Figure 2). The survival of the untreated WT and mutant strains remained unaffected (data not shown).

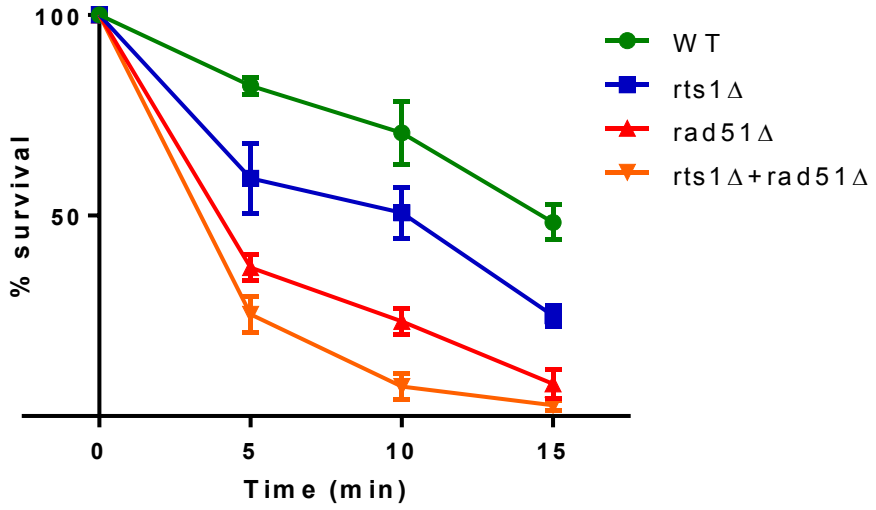

Figure 2. Survival Curve of Zeocin (25µg/ml) treated WT, *rts1*Δ, *rad51*Δ, *rts1Δrad51*Δ strains. All mutant strains showed sensitivity to Zeocin. The order of their sensitivity to Zeocin is as follows: WT< rts1Δ < rad51 Δ < rts1rad51Δ strains.

3.1.3 H_2O_2-induced oxidative stress reduces the nuclear recruitment of RTS1

The expression levels of *APN1* and *RTS1* (detected by anti-PAP) in the BY4741 WT and RTS1-TAP cells following H_2O_2 (0.5mM) treatment is shown in Figure 3. Treatment of BY4741 -WT as well as -RTS1-TAP cells with H_2O_2 did not produce significant changes in the expressional levels

of APN1. In contrast, treatment of BY4741-RTS1-TAP cells with H_2O_2 produced significant reduction in the levels of RTS1 at 60min post-H_2O_2 treatment.

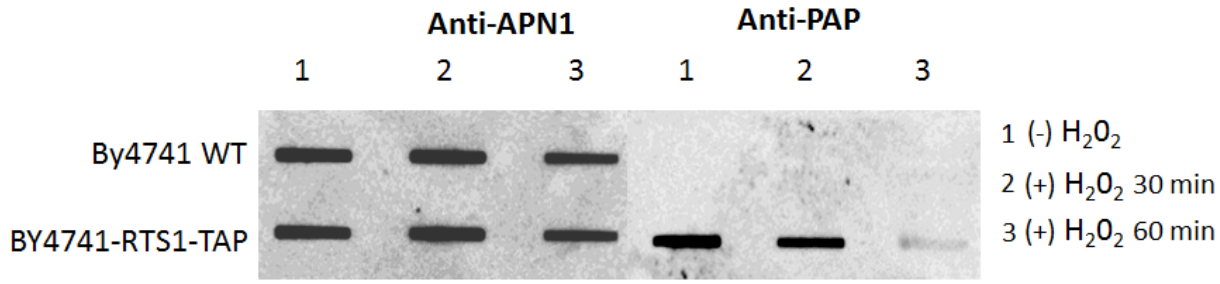

Figure 3. Effect of H_2O_2 treatment on the recruitment of Rts1 to DNA. Treatment of the BY4741–RTS1-TAP cells with H_2O_2 at 0.5mM reduced the expression levels of RTS1, but not APN1, at 60min post-treatment. No changes in the expression levels of APN1 were observed in the BY4741 WT cells following induction of oxidative stress with H_2O_2.

3.1.4 Protein Purification and Evaluation of RTS1-related proteins

The nuclear extracts were prepared from the BY4741–RTS1-TAP and BY4741-*rts1*Δ strains, and proteins from these extracts were purified using FPLC fraction method. Following FPLC, fourteen different fractions were selected and were then analyzed using Western Blot (data not shown). The fractions (#22 and #23) that showed the highest amount of Rts1 were subsequently loaded onto a 10% SDS polyacrylamide gel and stained with silver stain (Figure 4). Since, only fraction #23 showed significant changes, further experiments were performed only using this fraction. Specifically, fraction #23 showed a band loss at ~60 KDa (red arrow in WT lane) and generation of new bands at ~37 KDa (green arrow in mutant lane) in the BY4741-*rts1*Δ strain (Figure 4).

These specific bands were then cut and sent for mass spectrometry analysis in the laboratory of Ross Tomaino at Harvard University (Boston, MA). Although there were other band changes (blue arrow; ~80 – 100 KDa) observed in the analyzed fraction (#23), they were not included in the present study. The mass spectrometry analysis of the band lost and generated in the *rts1*Δ strain (Fraction #23) showed presence of various proteins. Table 2 and 3 shows the lists of highly expressed genes in the band lost and band generated, respectively, in the *rts1*Δ strain. Amongst the list of proteins determined, Cdc19 was found to be present in both the band lost (i.e., determined form the band present in the WT strain) as well as in the new band generated in the *rts1*Δ strain. The new band generated in the *rts1*Δ strain also showed higher expressional levels of *ENO1*.

3.1.5 Generation and validation of CDC19 and ENO1-related strains

In order to study the role of *CDC19* and *ENO1*, and its association with *RTS1*, we obtained BY4741-CDC19-TAP and BY4741-ENO1-TAP strains from Dr. Wurtele lab at Hôpital Maisonneuve-Rosemont (Montreal, QC). Following isolation of genomic DNA from the BY4741-CDC19-TAP and BY4741-ENO1-TAP strains, the *RTS1* gene was knocked-down using PCR (Table 1). The validity of *RTS1* knock-down was tested using the PCR end products. The DNA from BY4741 WT as well as BY4741-*rts1*Δ strains was included as experimental controls (Figure 5). Analysis of the end products demonstrated a band for WT strain at 2.2 Kbp, corresponding to *RTS1* (Figure 5). Since the *RTS1* was replaced with the *URA3* cassette, bands were observed at 1.2 Kbp for the BY4741-*rts1*Δ and BY4741-ENO-TAP-*rts1*Δ strains (Figure 5). This confirmed the successful generation of the BY4741-ENO-TAP-*rts1*Δ strain in our laboratory.

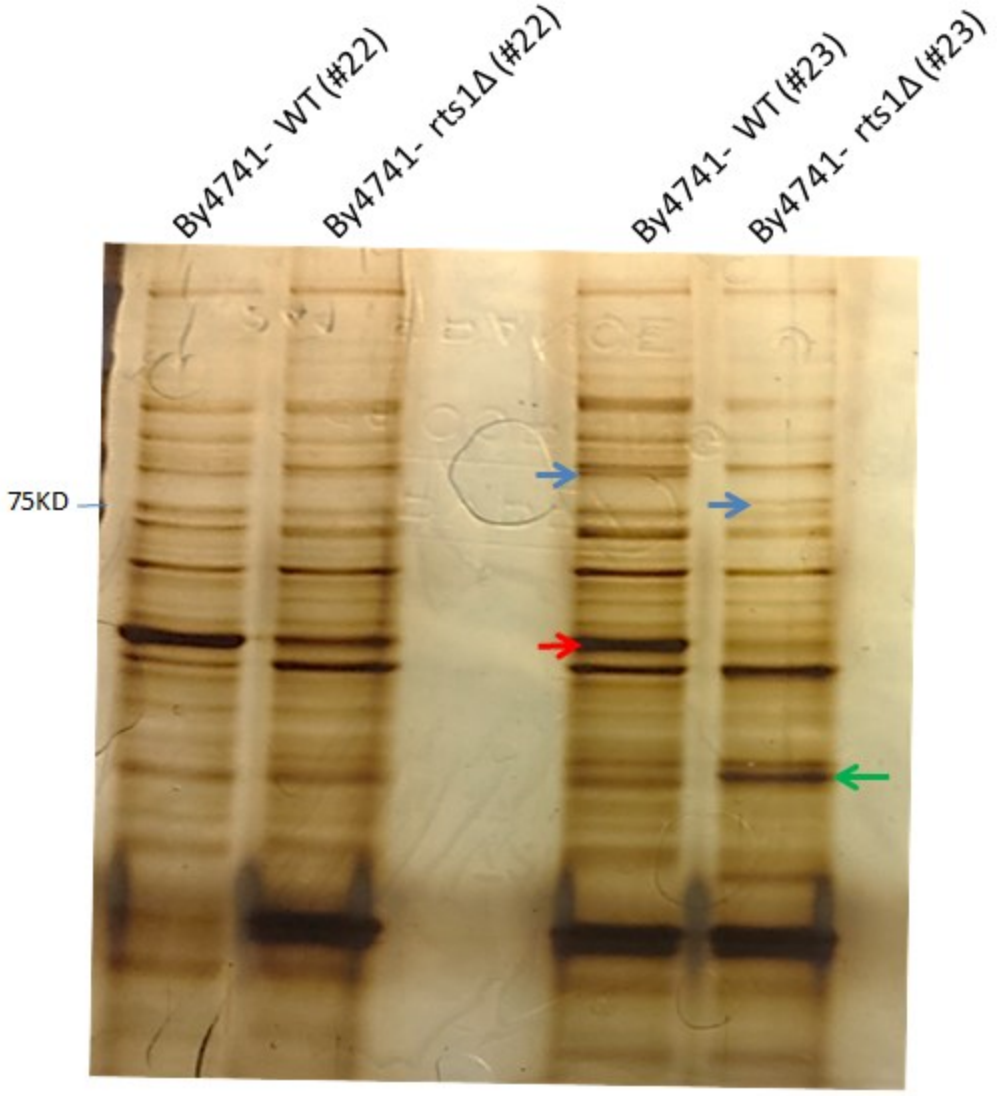

Figure 4. Silver stained polyacrylamide gel of fractions #22 and 23 extracted from BY4741 WT and –*rts1*Δ strains. Analysis of band changes showed generation of a new band (green arrow) and loss of a band (red arrow) in the *rts1*Δ strain. Blue arrow signifies other band changes that were not included in the present study.

Table 2. The list of highly expressed proteins of Fraction #23, determined using mass spectrometry, from the band lost (~60 KDa) in the *rts1*Δ strain.

#	Peptides	Gene Symbol	Reference
1	13	*CDC19*	*KPYK1_YEAST*
2	6	*ALD6*	*ALDH6_YEAST*
3	5	*SSA1*	*HSP71_YEAST*
4	5	*SSB1*	*HGP75_YEAST*

Table 3. The list of highly expressed proteins of Fraction #23, determined using mass spectrometry, from the new band generated (~37 KDa) in the *rts1*Δ strain.

#	Peptides	Gene Symbol	Reference
1	14	*ENO1*	*ENO1_YEAST*
2	6	*CDC19*	*KPYK1_YEAST*
3	4	*TEF1*	*EF1A_YEAST*
4	4	*SAH1*	*SAHH_YEAST*

However, observation of the band at 2.2 Kbp corresponding to *RTS1* in the BY4741-CDC19-TAP-*rts1*Δ strain suggests unsuccessful knock-down of the *RTS1* gene (Figure 5). The findings observed herein also were confirmed using Western blot (Figure 6A and B). Specifically, analysis of the western blot using the proteins isolated from the BY4741-CDC19-TAP and BY4741-CDC19-TAP-*rts1*Δ strains showed presence of non-specific bands at ~80 KDa, instead of the expected

bands at 55 KDa (Figure 6A). Hence, we decided to build a new strain using gap repair of the *CDC19* gene with Myc-Tag.

The *CDC19* gene was amplified using PCR technique with Platinum *PFX* DNA polymerase using the primers listed in Table1. The *CDC19* gene was cloned with MYC tag in the vector PTW438. The plasmid was transformed into D10b bacterial strain with chemical transformation. The colonies were grown overnight in Lb-Ampicillin liquid media and the plasmid (pCDC19-MYC) was extracted. Following extraction, pCDC19-MYC was transferred into BY4741 WT and *rts1*Δ strains, resulting in creation of BY4741-CDC19-Myc and BY4741-CDC19-Myc- *rts1*Δ strains. The strains generated herein were also validated using western blot, and findings showed specific bands as expected at 55 KDa (Figure 6B).

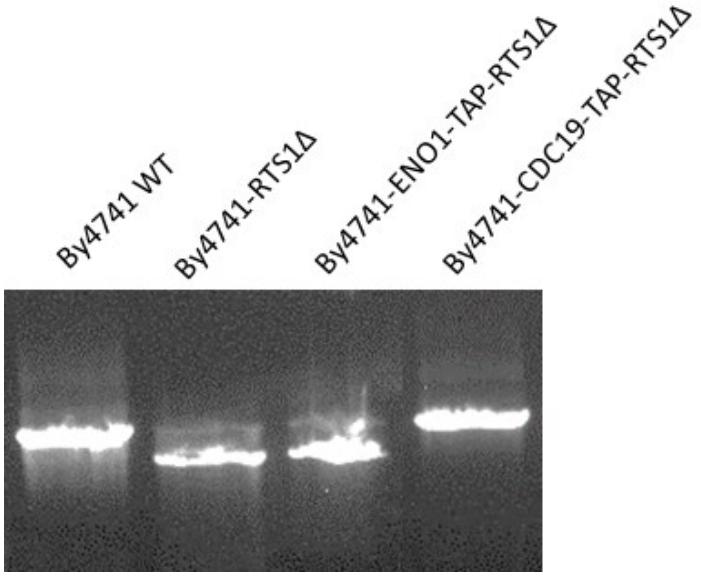

Figure 5. Analysis of PCR end products to confirm the deletion of *RTS1* gene. The WT strain showed a specific band at 2.2 Kbp, corresponding to *RTS1* gene. The appearance of band corresponding to URA3 cassette for the BY4741-*rts1*Δ and BY4741-ENO-TAP-*rts1*Δ strains

validates the deletion of the *RTS1* gene. In contrast, the appearance of band at 2.2 Kbp for the BY4741-CDC19-TAP-*rts1*Δ strain suggests unsuccessful deletion of the *RTS1* gene.

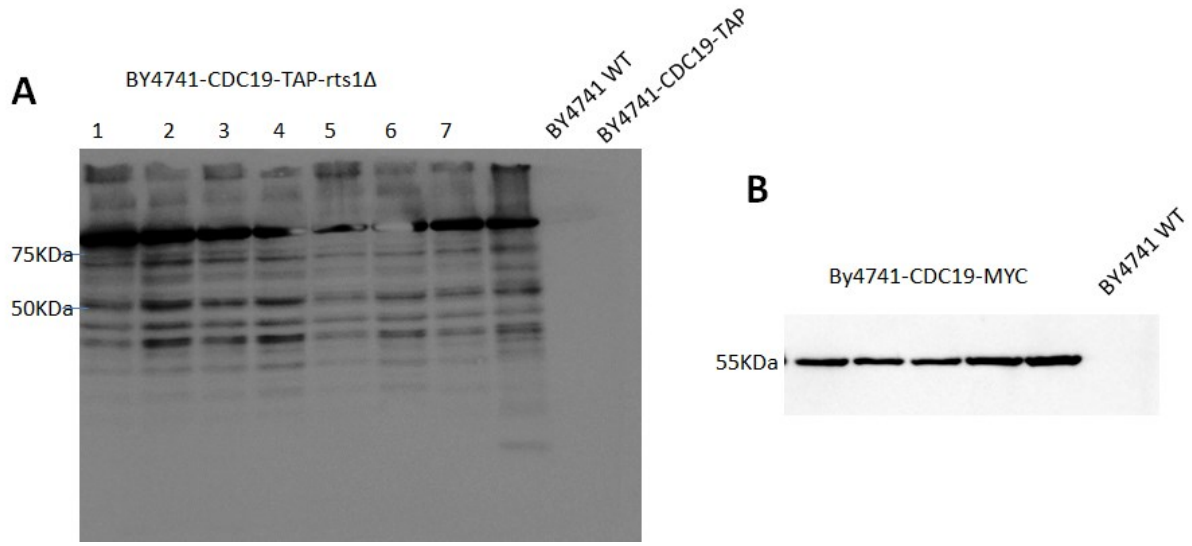

Figure 6. Validation of the BY4741 (A) CDC19-TAP and CDC19-TAP-*rts1*Δ, and (B) CDC19-MYC strains using anti-PAP and anti-Myc antibodies, respectively. Western blot of protein samples isolated from the CDC19-TAP and the CDC19-TAP-*rts1*Δ strains showed the presence of non-specific bands at ~80 KDa. The presence of bands at the expected size of 55 KDa in the CDC19-Myc strain, validates this created strain.

3.1.6 Deletion of RTS1 reduces the expression of ENO1

The nuclear proteins extracted from the BY4147 WT, -ENO1-TAP and –ENO1-TAP-*rts1*Δ strains were analyzed using western blot (Figure 7). There was a significant reduction in the expression of *ENO1*, as detected by anti-PAP antibody, in the ENO1-TAP-*rts1*Δ strain when compared to that of the ENO1-TAP strain. In contradiction to our findings herein, deletion of *RTS1* results in the appearance of a new band at ~37 KDa (as previously described in *Section 3.1.4*). Mass spectrometry analysis of this band showed *ENO1* as one of the up-regulated proteins (Table 3). On

a specific note, the band appeared in the *rts1*Δ strain showing increased expression of *ENO1* was at ~37 KDa, whereas the expression of ENO1-TAP herein was at ~67 KDa. The actual weight of *ENO*1 is ~47 KDa and TAP is ~19 KDa

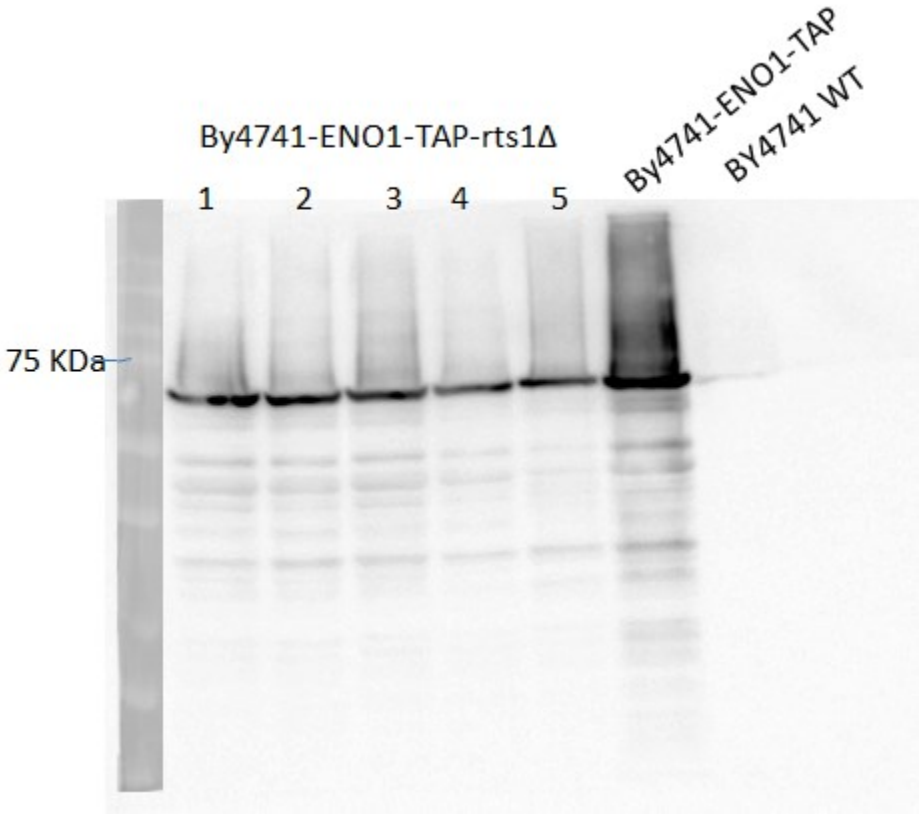

Figure 7. *rts1* Gene Deletion Reduces *ENO*1 Expression. Deletion of *RTS1* gene reduced the expressional levels of *ENO*1 in the ENO1-TAP-*rts1*Δ strain *c.f.* corresponding expressional levels in the ENO1-TAP strain.

3.1.7 Possible Role of RTS1 Gene in modulation the expression of CDC19

The differences in the expressional levels of *CDC19* was assessed and quantified in both untreated and Hygromycin treated BY4741-CDC19-Myc and BY4741-CDC19-Myc-*rts1*Δ strains (Figure 8 and 9). The expression level of the *CDC19*, as detected by the anti-Myc antibody, was found to be reduced in the untreated CDC19-Myc-*rts1*Δ strain, relative to that of the untreated CDC19-Myc

strain (Figure 8 and 9). Following treatment with hygromycin, there was an increase in the *CDC19* levels in the BY4741-CDC19-Myc strain *c.f.* untreated BY4741-CDC19-Myc strain (Figure 8 and 9). The observed up-regulation of *CDC19* levels following Hygromycin treatment in the BY4741-CDC19-Myc strain was found to be reduced in the Hygromycin treated BY4741-CDC19-Myc-*rts1*Δ strain (Figure 8 and 9). There were no differences in the CDC19 levels between the untreated and the Hygromycin treated BY4741-CDC19-Myc-*rts1*Δ strains (Figure 8 and 9). However, the percentage of reduction in the *CDC19* levels was higher for the Hygromycin treated BY4741-CDC19-Myc-*rts1*Δ relative to untreated BY4741-CDC19-Myc-*rts1*Δ strain, when compared to their respective untreated or treated BY4741-CDC19-Myc strains (Figure 9).

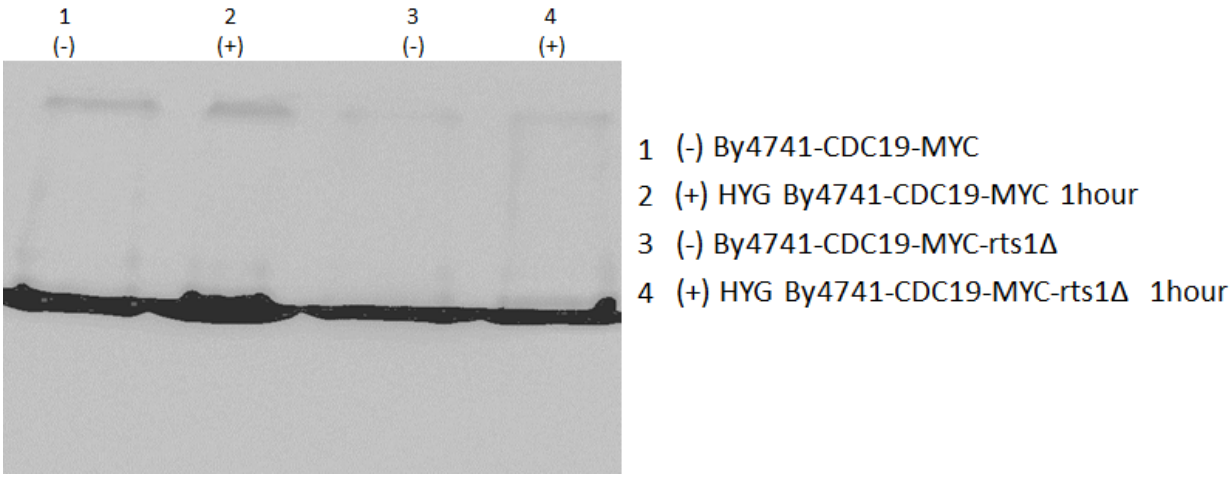

Figure 8. Expression levels of *CDC19* in untreated and Hygromycin (25 µg/ml)-treated BY4741-CDC19-Myc and BY4741-CDC19-Myc-*rts1*Δ strains. There was a reduction in the *CDC19* expression levels in both the untreated and Hygromycin treated CDC19-Myc-*rts1*Δ strain compared to their respective untreated and Hygromycin treated CDC19-Myc strain. Treatment of Hygromycin increased the *CDC19* levels in the CDC19-Myc strain, relative to the untreated

CDC19-Myc strain. In contrast, there were no differences in the *CDC19* levels between the untreated and Hygromycin treated CDC19-Myc-*rts1*Δ strains.

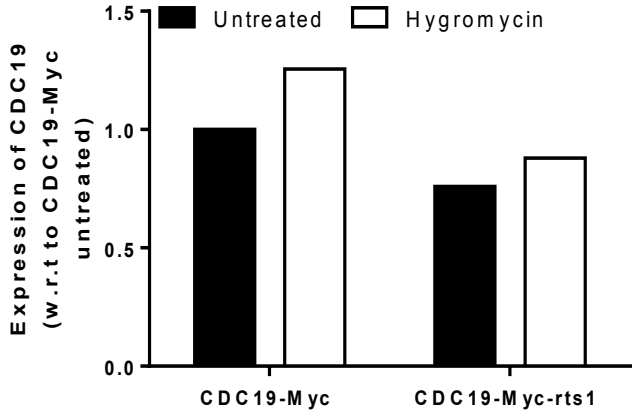

Figure 9. Quantification of the expression levels of *CDC19* in the untreated and Hygromycin (25 µg/ml)-treated BY4741-CDC19-MYC and BY4741-CDC19-MYC-*rts1*Δ strains.

CHAPTER 4. Second study results

4.1 Role of Histone H2A-E130A residue in recruiting Apn1

4.1.1. H2A-E130A mutant prevents localization of Apn1 to the nucleus

Figure 10 shows the representative immunocytochemistry images of the H2A WT and H2A-E130A cell strains stained for Apn1 and DAPI. The Apn1 was found to be localized in the nucleus of the H2A WT cell strains. In contrast, nuclear localization of Apn1 was not observed in the H2A-E130A cell strains.

The RADAR assay was also used to assess the expressional levels of Apn1 on the DNA of the H2A and H2A-E130A strains. Figure 10 shows the expression levels of Apn1 in the H2A WT and mutant strains. The expression levels of Apn1 was significantly higher in the H2A WT strain when compared to that of the H2A-E130A strain, validating an impaired attachment of the Apn1 to the DNA in the H2A-E130A strain. The expression levels of RNA polymerase II holoenzyme (RNAPII) served as an internal control for the experiment (Figure 11).

4.1.2. H2A- E130A mutant is sensitive to MMS

The sensitivity of various dilutions of H2A WT and mutant strains to MMS (0.0125 and 0.025 µg/ml) was assessed to understand the role of *Apn1* in DNA repair (Figure 12). MMS, a double strand breaking agent, was used to induce DNA-damage in the yeast strains (multiple dilutions) and spot test was used to assess the sensitivity of the cell strains. Our findings herein show that the H2A-E130A strain was comparatively more sensitive to MMS, in a dose-dependent manner, than the H2A WT strain (Figure 12).

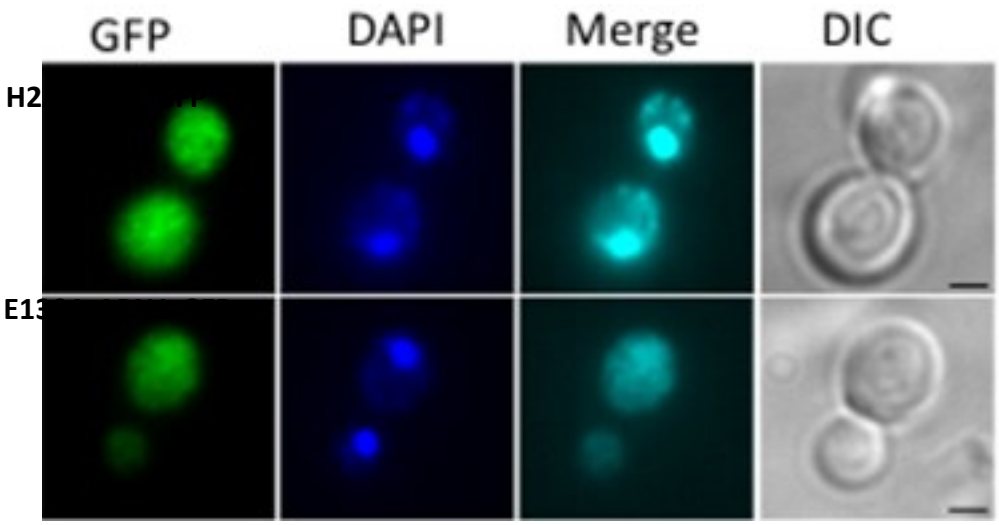

Figure 10. Differences in the nuclear localization of *APN1* in H2A and H2A-E130A cell strains. In these representative immunocytochemistry images (40X) of the H2A WT and H2A-E130A cell strains, GFP staining (green) represents *APN*1 and DAPI (blue) show nuclear staining. The merged images show the nuclear localization of *APN*1 in H2A WT, but not in H2A-E130 cell strains.

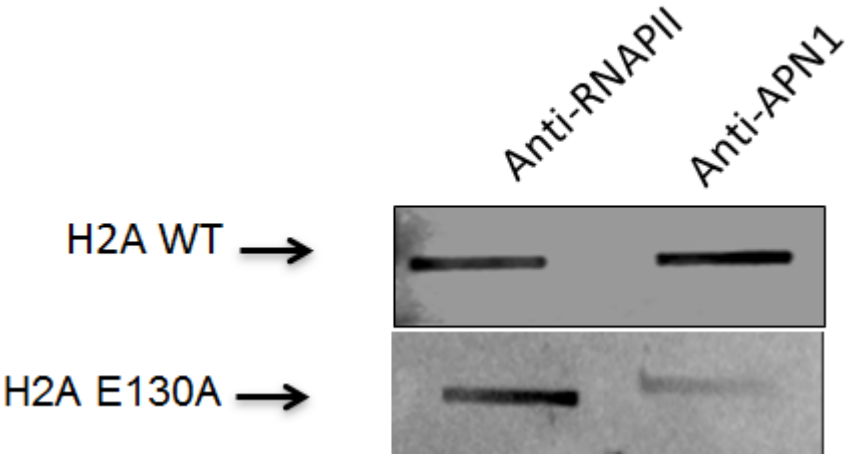

Figure 11. Expressional levels of *APN*1 in the nucleus of H2A and H2A-E130A strains. Increased expressional levels of *APN*1 were found in the H2A WT strain *c.f.* the respective levels in the mutant strain. In contrast, there were no differences in the expression levels of RNAPII (internal control) between the H2A WT and mutant strains.

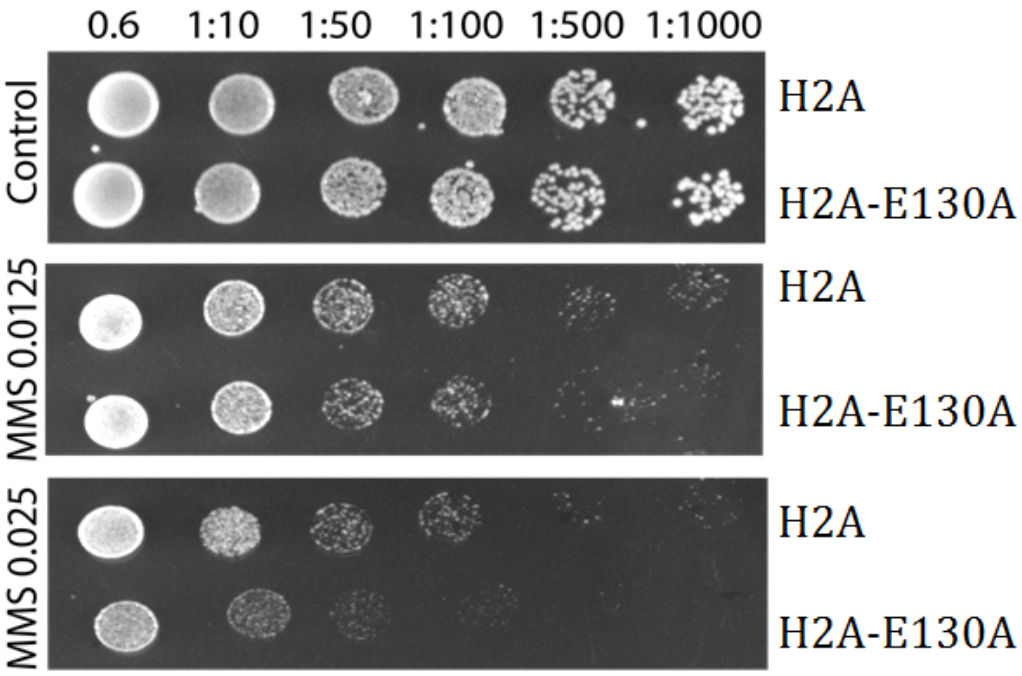

Figure 12. Sensitivity of H2A WT and H2A-E130A strains to MMS. MMS induced DNA damage in both the H2A WT and H2A-E130A cell strains in a dose-dependent manner, with H2A mutant strains demonstrating higher sensitivity to MMS than the H2A WT strain. Strains grown without addition of MMS did not show any DNA-damage, and thus served as a control for the experiment.

4.1.3. Knockdown of APN1 increases the sensitivity to MMS and decreases the life span of H2A-E130A strain.

Treatment of varying dilutions of H2A WT, H2A-*apn1*Δ, H2A-E130A and H2A-E130A-*apn1*Δ strains with MMS (0.0125 and 0.025 µg/ml) produced dose-dependent DNA-damage (Figure 13). Importantly, the degree of MMS-induced DNA damage was increased in the H2A-E130A-*apn1*Δ strain *c.f.* other H2A strains (Figure 13). Similar to earlier experiments described in *Section 4.1.2* (Figure 10), there was increased DNA damage in the H2A-E130A strain compared to H2A-WT strain (Figure 13). At the highest dose of MMS tested herein, the H2A-*apn1*Δ strain showed increased DNA-damage relative to that of the H2A WT strain (Figure 13).

Comparison of the survival rates of the untreated and MMS-treated strains is shown in Figure 14 A and B, respectively. There were no significant between-group differences in the survival of the non-treated strains. Although it was not significant, there was a trend towards reduction in the survival rate of the untreated H2A-E130A-*apn1*Δ strain (Figure 14A). In contrast, MMS treatment at 0.0125µg/ml significantly reduced the survival of both the H2A-*apn1*Δ and H2A-E130A-*apn1*Δ strains, relative to the survival rate of their respective APN1 WT strains (Figure 14B).

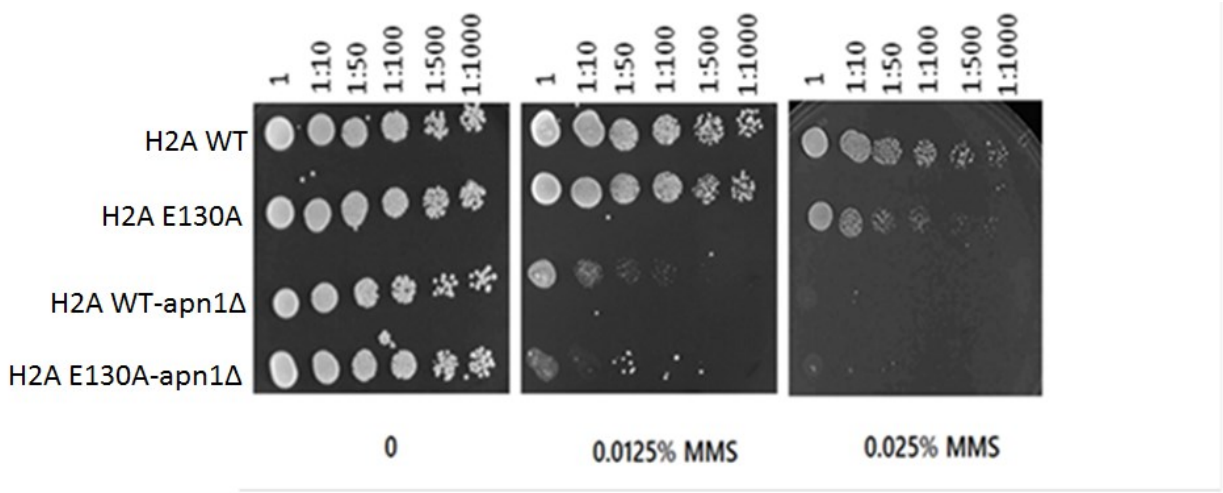

Figure 13. H2A-E130A mutant strain has increased sensitivity to MMS following deletion of *apn1*. The degree of MMS-induced DNA damage was assessed in the H2A WT, H2A-*apn1*Δ, H2A-E130A and H2A-E130A-*apn1*Δ strains of varying dilutions. MMS produced a dose-dependent DNA-damage response in the afore-mentioned strains. Importantly, the order of the degree of MMS-induced DNA damage is as follows: H2A WT < H2A-*apn1*Δ < H2A-E130A < H2A-E130A-*apn1*Δ.

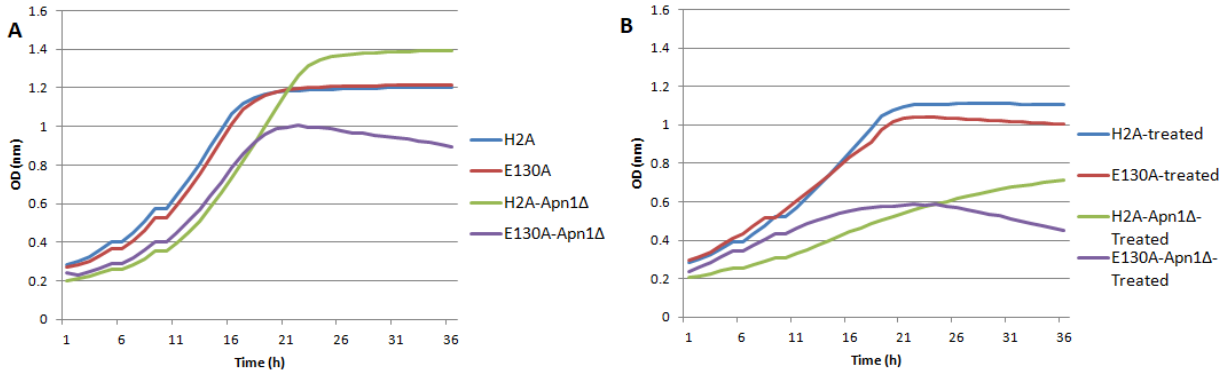

Figure 14. Deletion of *apn1* affects the survival rate of the H2A-E130A-*apn1*Δ strain. Panels A and B show the survival rate of the (A) untreated and (B) MMS (0.0125µg/ml)-treated H2A WT, H2A-E130A, H2A-*apn1*Δ and H2A-E130A-*apn1*Δ strains. There were no significant between-group differences in the survival of the non-treated strains, whilst a trend for reduction in the survival of the untreated H2A-E130A-*apn1*Δ strain was observed. The survival rate of MMS treated H2A-*apn1*Δ and H2A-E130A-*apn1*Δ was reduced when compared to the MMS-treated H2A WT and H2A-E130A strains.

CHAPTER 4. DISCUSSION and CONCLUSIONS

4. DISCUSSIONS and CONCLUSIONS

4.1 Role of RTS1 and its associated genes in regulating DNA-repair response

The present study shows a possible role for *Rts1* in the regulation of Zeocin- and hygromycin-related DNA-damage repair mechanisms, and associated of *RTS1* with various cell-cycle regulatory genes, viz. *APN1, CDC19* and *ENO1*. Specifically, treatment of wild-type (WT) and mutant BY4741 yeast strains with Zeocin, an antibiotic belonging to the Bleomycin family (Houser et al. 2001), demonstrated a reduction in the levels of *RTS1* and a corresponding decrease in the levels of *APN1*. Furthermore, analysis of the fast protein liquid chromatography (FPLC) fractions revealed associations of Rts1 with Cdc19 an Eno1. The associations of these genes with Rts1 were validated using experiments involving treatment of respective mutant and tandem affinity protein (TAP) or Myc tagged strains with hygromycin.

To date, numerous phosphatases and kinases have been implicated as major regulators of cell division processes (Bononi et al. 2011). Although kinases and phosphatases were thought merely as housekeeping enzymes, recent work have elucidated their critical role in the regulation of cell cycle processes (Janssens and Goris 2001, Virshup and Shenolikar 2009). One of the most versatile and important phosphatases involved in cell division is the protein phosphatase 2A (PP2A) (Jiang 2006). The regulatory role of PP2A in every stage of the cell cycle has been well-documented (see (Jiang 2006) for detailed review). More recently, PP2A has also been implicated in tumor suppression (Eichhorn, Creyghton, and Bernards 2009, O'Connor et al. 2017).

Rts1 protein is isoenzyme of B-regulatory subunit of the PP2A complex (Jiang 2006). The deletion of *RTS1* in various yeast strains, and subjected to various cellular stressors (e.g. oxidative stress,

DNA-damage etc.), have been shown to have defects in their growth, survival and cell cycle processes (Yang 2001). Previous works by others have also shown that yeast strains that lack *RTS1* are sensitive to temperature, ethanol and glycerol (Jiang 2006, Petty et al. 2016). Whilst the role of Rts1 in various cellular stress responses is known, the mechanisms underpinning the role of *RTS1* in modulating the expression of other cell cycle regulatory genes remains unclear.

In the present study, we evaluated the role of Rts1 in DNA-stress response following treatment of WT and mutant yeast strains with Zeocin and/or hydrogen peroxide (H_2O_2). Since the role of Apn1 has been well-established in DNA-related stress response and has a nuclear localization signal (Ramotar et al. 1993), we examined the expressional levels changes of *RTS1* alongside with *APN1*. Specifically, treatment of BY4741-WT and –RTS1-TAP strains with Zeocin showed a time-dependent reduction in the expressional levels of RTS1. Interestingly, the expression level of *APN1* was also found to be reduced following Zeocin treatment, indicating a possible cross-talk signalling between the Apn1 and Rts1. Additionally, the treatment of the BY4741-WT and –RTS1-TAP strains with H_2O_2 also resulted in a reduction in the expression levels of RTS1, but the expression levels of *APN1* herein remained unaffected. Since H_2O_2 is known to cause predominant single-strand DNA breaks (McDonald et al. 1993, Ribeiro, Corte-Real, and Johansson 2006), unlike Zeocin which causes DDSB (Chankova et al. 2007), it is possible that the functional role of Rts1, in response to single strand DNA breaks, is independent of Apn1. Future investigation to understand the differences in the functional role of Rts1 in single- and double-strand DNA break repair mechanism is warranted. Importantly, these data taken together with our findings showing time-dependent reduction in the survival of the Zeocin -treated BY4741-*rts1*Δ strains, suggests a role for Rts1 in the regulation of DNA-stress related repair mechanisms.

In addition to the *rts1* mutant, we also tested *rad51* mutant that has been previously shown to be sensitive to Hygromycin and Bleomycin (unpublished data). Our findings show a significant reduction in the survival of *rad51*Δ strains, following Zeocin treatment. Previous work in our laboratory has also demonstrated increased sensitivity of *rts1*Δ strains to Bleomycin (unpublished data). Importantly, the yeast strains that lacked both *RTS1* and *RAD51* displayed hypersensitivity to Zeocin treatment. Since, *rad51* has been previously associated with homologous recombination repair mechanism (HRR) (Krejci et al. 2012); it is possible that Rts1 may also have a role in the same pathway. Studies of replication fork stalling have also associated a pivotal role for Rts1 in the Rad51-depedent pathway (Ahn, Osman, and Whitby 2005).

The role of *RTS1* in modulating the expression of other cell-cycle regulatory genes remains unclear. Hence, we investigated the role of *RTS1* in regulation of other genes related to DNA repair pathway. Specifically, our findings from analysis of the FPLC fractions showed deletion of a band at ~60 kDa and generation of a new band at ~47 KDa for the *rts1*Δ strain. Mass spectrometry analysis of these bands revealed the proteins and their encoding genes. Amongst the proteins found, Cdc19 was found to be up-regulated in the band lost and Eno1 was found to be up-regulated in the new band generate in the *rts1*Δ strain. The *Cdc19* and *Eno1* genes have been previously implicated in glycolysis pathway (Williamson et al. 2012, Entelis et al. 2006), as well as a potential tumor marker that is associated with development and progression of various tumours (He et al. 2007). The *ENO1* has also additionally been shown to have a role in cellular growth control (Apte and Sarangarajan 2008). Although silver stained gel showed additional bands (~80 – 100 KDa),

they were not included in the present study and future investigation of these bands are warranted in near future to better understand the *RTS1*-associated genes.

Next, to understand association of Eno1 with Rts1, we obtained the BY4741-ENO1-TAP strain from Wurtele lab and subsequently created the BY4741-ENO1-TAP-*rts1*Δ strain. Following validation of the generated strain by analyzing the end products of the PCR, we investigated the changes in the expression levels of *ENO*1 following deletion of *RTS1*. Interestingly, the expression of *ENO*1 was found to be reduced following deletion of *RTS1*. In contrast to these findings, our mass spectrometry dataset of the new band generated in the *rts1*Δ strain showed an increase in the expression of *ENO*1. Future investigation of the contradictory observations is required to better understand these paradoxical findings.

In order to understand the association of Rts1 and Cdc19 in the DNA-repair process, we obtained BY4741-CDC19-TAP strain from Wurtele lab. However, analysis of the PCR end products of the DNA obtained from this strain showed unsuccessful deletion of *RTS1*. Analysis of the proteins extracted from the BY4741-CDC19-TAP-*rts1*Δ strain using western blot also showed non-specific bands for CDC19 at ~80 KDa instead of the expected band at 55 KDa. Hence, a new strain was generated involving a MYC tag, i.e. BY4741-CDC19- MYC, and subsequently a *rts1*Δ strain was created (BY4741-CDC19-MYC-*rts1*Δ). The deletion of *rts1* was confirmed in this strain using western blot approach. Finally, the differences in the expressional levels of *CDC19* was assessed in both untreated and Hygromycin treated BY4741-CDC19- MYC and BY4741-CDC19-MYC-*rts1*Δ strains. The expression levels of *CDC19* was found to be up-regulated in the CDC19-MYC strain treated with hygromycin, relative to *CDC19* levels in untreated CDC19-MYC strain. This

augmented *CDC19* expression level was reduced following deletion of *RTS1 gene* and treatment with hygromycin. The levels of *CDC19* were also found to be reduced in the untreated CDC19-MYC-*rts1*Δ strain *c.f.* untreated CDC19-MYC strain, validating our findings from the mass spectrometry. Nevertheless, a significant limitation in the interpretation of the findings is the absence of loading control in the western blot while assessing the expressional level changes of *CDC19.*

In summary, the present study shows a distinctive Apn1-dependant and Apn1-independent functional role for Rts1 in DNA-repair mechanisms involving DDSB and single strand DNA breaks, respectively. Furthermore, for the time, our findings show association of *RTS1* with that *CDC19* and *ENO1*, genes that have been previously implicated in the glycolysis pathways. Although, our findings show a possible role for Rts1 and Cdc19 in the hygromycin-related DNA-damage repair response, the absence of loading control in the experiment has hindered accurate interpretation of these findings. The paradoxical difference in the *ENO1* expression, when assessed using mass spectrometry and western blot technique, in the rts1Δ strain requires confirmation using additional experiments. Hence, further studies are required to better understand the association of Rts1 with that of Cdc19 and Eno1, and how their interaction affects the DNA-repair processes and/or cell cycle.

4.2 Role of Histone H2A-E130A residue in nuclear localization of Apn1

Our findings herein show that the Glu130 in the Histone H2A is required for the nuclear localization of Apn1. Additionally, the same residue is also responsible in determining the sensitivity of the H2A yeast strain to methyl methanesulfonate (MMS).

DNA lesion often occurs due to a variety of endogenous sources, such as non-enzymatic methylation, cytosine deamination and base oxidation, as well as exogenous sources (e.g., chemical oxidants, anti-cancer drugs, ionizing radiation etc.) (Meas, Smerdon, and Wyrick 2015). Failure to repair DNA lesions could result in chromosome rearrangement or loss, gene deletion and/or eventual death of cells, resulting in impaired replication, transcription and associated DNA damage-repair mechanisms (Hakem 2008). Excision repair mechanisms in the DNA remove the DNA lesions to avoid potential mutagenesis and carcinogenesis (Krokan and Bjoras 2013). However, predominant repairs to correct the DNA lesions occur via the base excision repair (BER) pathway (Krokan and Bjoras 2013). The BER pathway is initiated by creation of apurinic/apyrimidinic (AP) site following an N-glycosidic bond cleavage (Krokan and Bjoras 2013, Meas, Smerdon, and Wyrick 2015).

Apn1 protein plays a major role in the repair of apurinic/apyrimidinic (AP) sites (Boiteux and Guillet 2004). Previously, we have shown that the C-terminus of *APN1* has a region spanning nearly 82 amino acid residues which do not have a direct role in DNA repair (Ramotar et al. 1993). The distal part of the C-terminus contains two short segments (Clusters 1 and 2) that form a bipartite nuclear localization signal. It has been previously demonstrated that the N-terminal of histones also facilitates intra- and inter-nucleosomal interactions (Zheng and Hayes 2003). Furthermore, N-tail deletions of various histones have been shown to be sensitive to alkylating agents (Meas, Smerdon, and Wyrick 2015). Hence, we hypothesized that Histone mutant H2A-E130A residue may be involved in the recruitment of Apn1 via its interaction with the C-terminal of *APN*1.

To better understand the role of canonical core histones, such as the H2A, H2B, H3 and H4, we attached green fluorescent protein (GFP) on to the C-terminal chain of *APN*1. Subsequently, the APN1-GFP was introduced into a collection of histone mutant strains each expressing single amino acid changes of either histone H2A, H2B, H3 or H4 (unpublished data). Previous work in the laboratory has elucidates the role of various histone mutant libraries (unpublished data). The present study specifically investigated the role of H2A-E130A residue in the recruitment of Apn1 and its role in MMS-induced DNA damage response.

The H2A and mutant H2A-E130A strains were introduced with APN1-GFP. Immunocytochemical analysis of these strains revealed nuclear localization of APN1-GFP only in the H2A WT strain, but not in the H2A-E130A mutant strain. Additionally, RADAR assay was also used to quantify the expressional levels of *APN*1 in the H2A and H2A-E130A strains. Our findings herein showed higher *APN*1 levels in the H2A WT strain when compared to the H2A-E130A strain. These findings taken together suggest that the Glu130 residue of the H2A is required for the recruitment and nuclear localization of Apn1.

The accumulation of AP sites in the nucleus of yeast strains due to deficiency in the recruitment of Apn1 has been previously shown to affect the sensitivity of the strains to DNA damaging agents such as MMS and Hygromycin (Ma, Resnick, and Gordenin 2008, Ramotar et al. 1993, Wemhoff et al. 2016). In support of this notion, the treatment of H2A-E130A strain, which showed reduced recruitment of Apn1, displayed sensitivity to MMS, in a dose-dependent manner, compared to the H2A WT strain. On a specific note, the recruitment of Apn1 has also been demonstrated to be

required for mitochondrial DNA repair, in addition to nuclear DNA repair, following MMS treatment (Acevedo-Torres et al. 2009).

Finally, we compared the effects of reduced Apn1 nuclear recruitment and complete absence of *APN*1 (deletion of *APN1 gene*), on the sensitivity and life span of the untreated and the MMS-treated H2A WT and H2A-E130A strains. In line with our hypothesis, both untreated as well as MMS-treated H2A-E130A-*apn1*Δ strains displayed hypersensitivity and reduced growth rate. Our findings herein are reminiscent of previous work by others showing hypersensitivity and reduced growth rate of MMS-*apn1*Δ strains (Ma, Resnick, and Gordenin 2008, Wemhoff et al. 2016). Interestingly, the growth rate of the MMS-treated H2A-*apn1*Δ was also found to be reduced, suggesting the importance of *APN1* in the MMS-induced DNA-damage repair.

In conclusion, our findings herein show preliminary data to support the role of Glu130 residue of Histone H2A in the nuclear localization of Apn1. Importantly, our pilot data also show the robust role of the Glu130 in determining the sensitivity as well as the growth rate of the H2A strain to MMS. Time limitations precluded the use of FPLC and subsequent mass spectrometry analysis of the *APN1*-related genes. Future investigation of the *APN1*-related genes will facilitate better understanding of the role of Apn1 and its associated genes in regulating the repair mechanisms following double strand DNA breaks induced by alkylating agents.

References

Acevedo-Torres, K., S. Fonseca-Williams, S. Ayala-Torres, and C. A. Torres-Ramos. 2009a. "Requirement of the Saccharomyces cerevisiae APN1 gene for the repair of mitochondrial DNA alkylation damage." *Environ Mol Mutagen* 50 (4):317-27. doi: 10.1002/em.20462.

Acevedo-Torres, K., S. Fonseca-Williams, S. Ayala-Torres, and C. A. Torres-Ramos. 2009b. "Requirement of the Saccharomyces cerevisiae APN1 Gene for the Repair of Mitochondrial DNA Alkylation Damage." *Environmental and Molecular Mutagenesis* 50 (4):317-327. doi: 10.1002/em.20462.

Ahn, J. S., F. Osman, and M. C. Whitby. 2005. "Replication fork blockage by RTS1 at an ectopic site promotes recombination in fission yeast." *Embo Journal* 24 (11):2011-2023. doi: 10.1038/sj.emboj.7600670.

Apte, Shireesh, and Rangaprasad Sarangarajan. 2008. *Cellular respiration and carcinogenesis*: Springer Science & Business Media.

Artiles, Karen, Stephanie Anastasia, Derek McCusker, and Douglas R Kellogg. 2009. "The Rts1 regulatory subunit of protein phosphatase 2A is required for control of G1 cyclin transcription and nutrient modulation of cell size." *PLoS genetics* 5 (11):e1000727.

Attfield, Paul V. 1997. "Stress tolerance: the key to effective strains of industrial baker's yeast." *Nature biotechnology* 15 (13):1351.

Aunoble, BÉNÉDICTE, R Sanches, E Didier, and YJ Bignon. 2000. "Major oncogenes and tumor suppressor genes involved in epithelial ovarian cancer." *International journal of oncology* 16 (3):567-643.

Bjornsti, M. A. 2002. "Cancer therapeutics in yeast." *Cancer Cell* 2 (4):267-273. doi: Doi 10.1016/S1535-6108(02)00160-5.

Boiteux, S., and M. Guillet. 2004. "Abasic sites in DNA: repair and biological consequences in Saccharomyces cerevisiae." *DNA Repair (Amst)* 3 (1):1-12.

Boiteux, S., and S. Jinks-Robertson. 2013. "DNA Repair Mechanisms and the Bypass of DNA Damage in Saccharomyces cerevisiae." *Genetics* 193 (4):1025-1064. doi: 10.1534/genetics.112.145219.

Bonisch, C., and S. B. Hake. 2012. "Histone H2A variants in nucleosomes and chromatin: more or less stable?" *Nucleic Acids Research* 40 (21):10719-10741. doi: 10.1093/nar/gks865.

Bononi, A., C. Agnoletto, E. De Marchi, S. Marchi, S. Patergnani, M. Bonora, C. Giorgi, S. Missiroli, F. Poletti, A. Rimessi, and P. Pinton. 2011. "Protein kinases and phosphatases in the control of cell fate." *Enzyme Res* 2011:329098. doi: 10.4061/2011/329098.

Bugaut, Hélène, Mélanie Bruchard, Hélène Berger, Valentin Derangère, Ludivine Odoul, Romain Euvrard, Sylvain Ladoire, Fanny Chalmin, Frédérique Végran, and Cédric Rébé. 2013. "Bleomycin exerts ambivalent antitumor immune effect by triggering both immunogenic cell death and proliferation of regulatory T cells." *PLoS One* 8 (6):e65181.

Chalissery, J., D. Jalal, Z. Al-Natour, and A. H. Hassan. 2017. "Repair of Oxidative DNA Damage in Saccharomyces cerevisiae." *DNA Repair* 51:2-13. doi: 10.1016/j.dnarep.2016.12.010.

Chan, Leon Y, and Angelika Amon. 2009. "The protein phosphatase 2A functions in the spindle position checkpoint by regulating the checkpoint kinase Kin4." *Genes & development* 23 (14):1639-1649.

Chankova, S. G., E. Dimova, M. Dimitrova, and P. E. Bryant. 2007. "Induction of DNA double-strand breaks by Zeocin in Chlamydomonas reinhardtii and the role of increased DNA double-strand breaks rejoining in the formation of an adaptive response." *Radiat Environ Biophys* 46 (4):409-16. doi: 10.1007/s00411-007-0123-2.

Chen, J. Y., M. K. Ghorai, G. Kenney, and J. Stubbe. 2008. "Mechanistic studies on bleomycin-mediated DNA damage: multiple binding modes can result in double-stranded DNA cleavage." *Nucleic Acids Research* 36 (11):3781-3790. doi: 10.1093/nar/gkn302.

Chevallet, M., S. Luche, and T. Rabilloud. 2006. "Silver staining of proteins in polyacrylamide gels." *Nat Protoc* 1 (4):1852-8. doi: 10.1038/nprot.2006.288.

Dolinski, K., and D. Botstein. 2007. "Orthology and functional conservation in eukaryotes." *Annual Review of Genetics* 41:465-507. doi: 10.1146/annurev.genet.40.110405.090439.

Eichhorn, Pieter JA, Menno P Creyghton, and René Bernards. 2009. "Protein phosphatase 2A regulatory subunits and cancer." *Biochimica et Biophysica Acta (BBA)-Reviews on Cancer* 1795 (1):1-15.

Entelis, N., I. Brandina, P. Kamenski, I. A. Krasheninnikov, R. P. Martin, and I. Tarassov. 2006. "A glycolytic enzyme, enolase, is recruited as a cofactor of tRNA targeting toward mitochondria in Saccharomyces cerevisiae." *Genes & Development* 20 (12):1609-1620. doi: 10.1101/gad.385706.

Ferlay, J., I. Soerjomataram, R. Dikshit, S. Eser, C. Mathers, M. Rebelo, D. M. Parkin, D. Forman, and F. Bray. 2015. "Cancer incidence and mortality worldwide: Sources, methods and major patterns in GLOBOCAN 2012." *International Journal of Cancer* 136 (5):E359-E386. doi: 10.1002/ijc.29210.

Fidler, M. M., S. Gupta, I. Soerjomataram, J. Ferlay, E. Steliarova-Foucher, and F. Bray. 2017. "Cancer incidence and mortality among young adults aged 20-39 years worldwide in 2012: a population-based study." *Lancet Oncology* 18 (12):1579-1589. doi: 10.1016/S1470-2045(17)30677-0.

Folch-Mallol, JL, A Garay-Arroyo, F Lledias, and AA Robles Covarrubias. 2004. "The stress response in the yeast Saccharomyces cerevisiae." *Revista latinoamericana de microbiologia* 46 (1-2):24-46.

Gatenby, Robert A. 2009. "A change of strategy in the war on cancer." *Nature* 459 (7246):508.

Hakem, R. 2008. "DNA-damage repair; the good, the bad, and the ugly." *Embo Journal* 27 (4):589-605. doi: 10.1038/emboj.2008.15.

Hanahan, D., and R. A. Weinberg. 2011. "Hallmarks of Cancer: The Next Generation." *Cell* 144 (5):646-674. doi: 10.1016/j.cell.2011.02.013.

He, P., T. Naka, S. Serada, M. Fujimoto, T. Tanaka, S. Hashimoto, Y. Shima, T. Yamadori, H. Suzuki, T. Hirashima, K. Matsui, H. Shiono, M. Okumura, T. Nishida, I. Tachibana, N. Norioka, S. Norioka, and I. Kawase. 2007. "Proteomics-based identification of alpha-enolase as a tumor antigen in non-small lung cancer." *Cancer Sci* 98 (8):1234-40. doi: 10.1111/j.1349-7006.2007.00509.x.

Hoeijmakers, J. H. J. 2001. "Genome maintenance mechanisms for preventing cancer." *Nature* 411 (6835):366-374. doi: Doi 10.1038/35077232.

Houser, S., S. Koshlatyi, T. Lu, T. Gopen, and J. Bargonetti. 2001. "Camptothecin and Zeocin can increase p53 levels during all cell cycle stages." *Biochemical and Biophysical Research Communications* 289 (5):998-1009. doi: 10.1006/bbrc.2001.6073.

Janssens, V., and J. Goris. 2001a. "Protein phosphatase 2A: a highly regulated family of serine/threonine phosphatases implicated in cell growth and signalling." *Biochemical Journal* 353:417-439. doi: Doi 10.1042/0264-6021:3530417.

Janssens, Veerle, and Jozef Goris. 2001b. "Protein phosphatase 2A: a highly regulated family of serine/threonine phosphatases implicated in cell growth and signalling." *Biochemical Journal* 353 (Pt 3):417.

Jiang, Y. 2006. "Regulation of the cell cycle by protein phosphatase 2A in Saccharomyces cerevisiae." *Microbiol Mol Biol Rev* 70 (2):440-9. doi: 10.1128/MMBR.00049-05.

Johnson, R. E., C. A. Torres-Ramos, T. Izumi, S. Mitra, S. Prakash, and L. Prakash. 1998. "Identification of APN2, the Saccharomyces cerevisiae homolog of the major human AP endonuclease HAP1, and its role in the repair of abasic sites." *Genes & Development* 12 (19):3137-3143. doi: DOI 10.1101/gad.12.19.3137.

Kim, J. A., J. Y. Hsu, M. M. Smith, and C. D. Allis. 2012. "Mutagenesis of pairwise combinations of histone amino-terminal tails reveals functional redundancy in budding yeast." *Proceedings of the National Academy of Sciences of the United States of America* 109 (15):5779-5784. doi: 10.1073/pnas.1203453109.

Kitanovic, A., T. Walther, M. O. Loret, J. Holzwarth, I. Kitanovic, F. Bonowski, N. V. Bui, J. M. Francois, and S. Wolfl. 2009. "Metabolic response to MMS-mediated DNA damage in Saccharomyces cerevisiae is dependent on the glucose concentration in the medium." *Fems Yeast Research* 9 (4):535-551. doi: 10.1111/j.1567-1364.2009.00505.x.

Krejci, L., V. Altmannova, M. Spirek, and X. Zhao. 2012. "Homologous recombination and its regulation." *Nucleic Acids Res* 40 (13):5795-818. doi: 10.1093/nar/gks270.

Krokan, H. E., and M. Bjoras. 2013. "Base Excision Repair." *Cold Spring Harbor Perspectives in Biology* 5 (4). doi: ARTN a012583

10.1101/cshperspect.a012583.

Lee, J. K., Y. L. Choi, M. Kwon, and P. J. Park. 2016. "Mechanisms and Consequences of Cancer Genome Instability: Lessons from Genome Sequencing Studies." *Annual Review of Pathology: Mechanisms of Disease, Vol 11* 11:283-312. doi: 10.1146/annurev-pathol-012615-044446.

Lee, Y. C. A., and M. Hashibe. 2014. "Tobacco, Alcohol, and Cancer in Low and High Income Countries." *Annals of Global Health* 80 (5):378-383. doi: 10.1016/j.aogh.2014.09.010.

Li, Xinghai, and David M Virshup. 2002. "Two conserved domains in regulatory B subunits mediate binding to the A subunit of protein phosphatase 2A." *The FEBS Journal* 269 (2):546-552.

Lippert, T. H., H. J. Ruoff, and M. Volm. 2011. "Current Status of Methods to Assess Cancer Drug Resistance." *International Journal of Medical Sciences* 8 (3):245-253. doi: Doi 10.7150/Ijms.8.245.

Litwin, I., D. Dziadkowiec, and R. Wysocki. 2013. "Oxidative stress and replication-independent DNA breakage induced by arsenic in Saccharomyces cerevisiae." *Yeast* 30:68-68.

Lou, H., and M. Dean. 2007. "Targeted therapy for cancer stem cells: the patched pathway and ABC transporters." *Oncogene* 26 (9):1357-1360. doi: 10.1038/sj.onc.1210200.

Ma, W., M. A. Resnick, and D. A. Gordenin. 2008. "Apn1 and Apn2 endonucleases prevent accumulation of repair-associated DNA breaks in budding yeast as revealed by direct chromosomal analysis." *Nucleic Acids Res* 36 (6):1836-46. doi: 10.1093/nar/gkm1148.

McDonald, R. J., L. C. Pan, J. A. St George, D. M. Hyde, and J. M. Ducore. 1993. "Hydrogen peroxide induces DNA single strand breaks in respiratory epithelial cells." *Inflammation* 17 (6):715-22.

Meads, M. B., R. A. Gatenby, and W. S. Dalton. 2009. "Environment-mediated drug resistance: a major contributor to minimal residual disease." *Nature Reviews Cancer* 9 (9):665-A674. doi: 10.1038/nrc2714.

Meas, R., M. J. Smerdon, and J. J. Wyrick. 2015a. "The amino-terminal tails of histones H2A and H3 coordinate efficient base excision repair, DNA damage signaling and postreplication repair in Saccharomyces cerevisiae." *Nucleic Acids Research* 43 (10):4990-5001. doi: 10.1093/nar/gkv372.

Meas, R., M. J. Smerdon, and J. J. Wyrick. 2015b. "The amino-terminal tails of histones H2A and H3 coordinate efficient base excision repair, DNA damage signaling and postreplication repair in Saccharomyces cerevisiae." *Nucleic Acids Res* 43 (10):4990-5001. doi: 10.1093/nar/gkv372.

Migliore, L., and F. Coppede. 2002. "Genetic and environmental factors in cancer and neurodegenerative diseases." *Mutation Research-Reviews in Mutation Research* 512 (2-3):135-153. doi: Pii S1383-5742(02)00046-7

Doi 10.1016/S1383-5742(02)00046-7.

Narang, Ajit S., and Divyakant S. Desai. 2009. "Anticancer Drug Development." In *Pharmaceutical Perspectives of Cancer Therapeutics*, edited by Yi Lu and Ram I. Mahato, 49-92. New York, NY: Springer US.

Nassour, H., Z. Wang, A. Saad, A. Papaluca, N. Brosseau, B. Affar el, M. A. Alaoui-Jamali, and D. Ramotar. 2016. "Peroxiredoxin 1 interacts with and blocks the redox factor APE1 from activating interleukin-8 expression." *Sci Rep* 6:29389. doi: 10.1038/srep29389.

Nussbaumer, S., P. Bonnabry, J. L. Veuthey, and S. Fleury-Souverain. 2011. "Analysis of anticancer drugs: A review." *Talanta* 85 (5):2265-2289. doi: 10.1016/j.talanta.2011.08.034.

O'Connor, Caitlin M, Abbey Perl, Daniel Leonard, Jaya Sangodkar, and Goutham Narla. 2017. "Therapeutic Targeting of PP2A." *The international journal of biochemistry & cell biology*.

Paddison, P. J., and G. J. Hannon. 2002. "RNA interference: the new somatic cell genetics?" *Cancer Cell* 2 (1):17-23. doi: Doi 10.1016/S1535-6108(02)00092-2.

Parsa, N. 2012. "Environmental Factors Inducing Human Cancers." *Iranian Journal of Public Health* 41 (11):1-9.

Petty, E. L., A. Lafon, S. L. Tomlinson, B. A. Mendelsohn, and L. Pillus. 2016. "Promotion of Cell Viability and Histone Gene Expression by the Acetyltransferase Gcn5 and the Protein Phosphatase PP2A in Saccharomyces cerevisiae." *Genetics* 203 (4):1693-+. doi: 10.1534/genetics.116.189506.

Pinson, B., I. Sagot, and B. Daignan-Fornier. 2000. "Identification of genes affecting selenite toxicity and resistance in Saccharomyces cerevisiae." *Molecular Microbiology* 36 (3):679-687. doi: DOI 10.1046/j.1365-2958.2000.01890.x.

Popoff, S. C., A. I. Spira, A. W. Johnson, and B. Demple. 1990. "Yeast Structural Gene (Apn1) for the Major Apurinic Endonuclease - Homology to Escherichia-Coli Endonuclease-Iv." *Proceedings of the National Academy of Sciences of the United States of America* 87 (11):4193-4197. doi: DOI 10.1073/pnas.87.11.4193.

Ramotar, D, C Kim, R Lillis, and B Demple. 1993. "Intracellular localization of the Apn1 DNA repair enzyme of Saccharomyces cerevisiae. Nuclear transport signals and biological role." *Journal of Biological Chemistry* 268 (27):20533-20539.

Ramotar, D., S. C. Popoff, E. B. Gralla, and B. Demple. 1991. "Cellular Role of Yeast Apn1 Apurinic Endonuclease 3'-Diesterase - Repair of Oxidative and Alkylation DNA Damage and Control of Spontaneous Mutation." *Molecular and Cellular Biology* 11 (9):4537-4544. doi: Doi 10.1128/Mcb.11.9.4537.

Ribeiro, G. F., M. Corte-Real, and B. Johansson. 2006. "Characterization of DNA damage in yeast apoptosis induced by hydrogen peroxide, acetic acid, and hyperosmotic shock." *Mol Biol Cell* 17 (10):4584-91. doi: 10.1091/mbc.E06-05-0475.

Richmond, T. J. 1999. "Hot papers - Crystal structure - Crystal structure of the nucleosome core particle at 2.8 angstrom resolution by K. Luger, A.W. Mader, R.K. Richmond, D.F. Sargent, T.J. Richmond - Comments." *Scientist* 13 (23):15-15.

Sherman, F. 2002. "Getting started with yeast." *Guide to Yeast Genetics and Molecular and Cell Biology, Pt B* 350:3-41. doi: Doi 10.1016/S0076-6879(02)50954-X.

Simon, J. A., P. Szankasi, D. K. Nguyen, C. Ludlow, H. M. Dunstan, C. J. Roberts, E. L. Jensen, L. H. Hartwell, and S. H. Friend. 2000. "Differential toxicities of anticancer agents among DNA repair and checkpoint mutants of Saccharomyces cerevisiae." *Cancer Research* 60 (2):328-333.

Sisakova, A., V. Altmannova, M. Sebesta, and L. Krejci. 2017. "Role of PCNA and RFC in promoting Mus81-complex activity." *BMC Biol* 15 (1):90. doi: 10.1186/s12915-017-0429-8.

Soria, G., S. E. Polo, and G. Almouzni. 2012. "Prime, Repair, Restore: The Active Role of Chromatin in the DNA Damage Response." *Molecular Cell* 46 (6):722-734. doi: 10.1016/j.molcel.2012.06.002.

Sud, A., B. Kinnersley, and R. S. Houlston. 2017. "Genome-wide association studies of cancer: current insights and future perspectives." *Nature Reviews Cancer* 17 (11):692-704. doi: 10.1038/nrc.2017.82.

Torre, L. A., F. Bray, R. L. Siegel, J. Ferlay, J. Lortet-Tieulent, and A. Jemal. 2015. "Global Cancer Statistics, 2012." *Ca-a Cancer Journal for Clinicians* 65 (2):87-108. doi: 10.3322/caac.21262.

Ullah, M. F. 2008. "Cancer Multidrug Resistance (MDR): A Major Impediment to Effective Chemotherapy." *Asian Pacific Journal of Cancer Prevention* 9 (1):1-6.

Venkatesh, S., and J. L. Workman. 2015. "Histone exchange, chromatin structure and the regulation of transcription." *Nature Reviews Molecular Cell Biology* 16 (3):178-189. doi: 10.1038/nrm3941.

Virshup, David M, and Shirish Shenolikar. 2009. "From promiscuity to precision: protein phosphatases get a makeover." *Molecular cell* 33 (5):537-545.

Wemhoff, S., R. Klassen, A. Beetz, and F. Meinhardt. 2016. "DNA Damage Responses Are Induced by tRNA Anticodon Nucleases and Hygromycin B." *PLoS One* 11 (7):e0157611. doi: 10.1371/journal.pone.0157611.

Williamson, Elizabeth A, Justin W Wray, Pranshu Bansal, and Robert Hromas. 2012. "Overview for the histone codes for DNA repair." In *Progress in molecular biology and translational science*, 207-227. Elsevier.

Williamson, T., D. Adiamah, J. M. Schwartz, and L. Stateva. 2012. "Exploring the genetic control of glycolytic oscillations in Saccharomyces cerevisiae." *BMC Syst Biol* 6:108. doi: 10.1186/1752-0509-6-108.

Yang, Haifeng. 2001. "Functional study of RTS1 and CDC55, two genes encoding regulatory subunits of protein phosphatase 2A in Saccharomyces cerevisiae."

Yang, X., J. Fan, A. A. Ishchenko, D. Patel, M. K. Saparbaev, and D. Ramotar. 2012. "Functional characterization of the Caenorhabditis elegans DNA repair enzyme APN-1." *DNA Repair (Amst)* 11 (10):811-22. doi: 10.1016/j.dnarep.2012.06.009.

You, H. J., R. L. Swanson, C. Harrington, A. H. Corbett, S. Jinks-Robertson, S. Senturker, S. S. Wallace, S. Boiteux, M. Dizdaroglu, and P. W. Doetsch. 1999. "Saccharomyces cerevisiae Ntg1p and Ntg2p: Broad specificity N-glycosylases for the repair of oxidative DNA damage in the nucleus and mitochondria." *Biochemistry* 38 (35):11298-11306. doi: Doi 10.1021/Bi991121i.

Zahreddine, H., and K. L. B. Borden. 2013. "Mechanisms and insights into drug resistance in cancer." *Frontiers in Pharmacology* 4. doi: Artn 28

10.3389/Fphar.2013.00028.

Zapata, Jessica, Noah Dephoure, Tracy MacDonough, Yaxin Yu, Emily J Parnell, Meghan Mooring, Steven P Gygi, David J Stillman, and Douglas R Kellogg. 2014. "PP2ARts1 is a master regulator of pathways that control cell size." *J Cell Biol* 204 (3):359-376.

Zheng, C., and J. J. Hayes. 2003a. "Intra- and inter-nucleosomal protein-DNA interactions of the core histone tail domains in a model system." *J Biol Chem* 278 (26):24217-24. doi: 10.1074/jbc.M302817200.

Zheng, C. Y., and J. J. Hayes. 2003b. "Intra- and inter-nucleosomal protein-DNA interactions of the core histone tail domains in a model system." *Journal of Biological Chemistry* 278 (26):24217-24224. doi: 10.1074/jbc.M302817200.

Zhong, G. W., P. Jiang, W. R. Qiao, Y. W. Zhang, W. F. Wei, and L. Lu. 2014. "Protein Phosphatase 2A (PP2A) Regulatory Subunits ParA and PabA Orchestrate Septation and Conidiation and Are Essential for PP2A Activity in Aspergillus nidulans." *Eukaryotic Cell* 13 (12):1494-1506. doi: 10.1128/Ec.00201-14.